Liquid Fragility and the Glass Transition in Water and Aqueous Solutions

C. A. Angell

Department of Chemistry and Biochemistry, Arizona State University, Tempe, Arizona 85287-1604

Received September 18, 2001

Contents

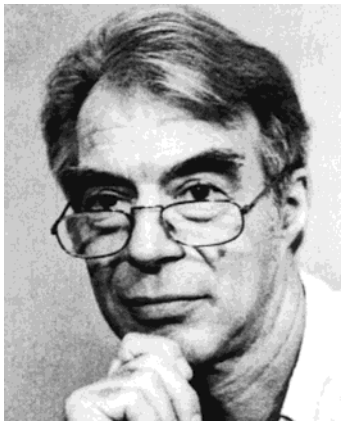

C. A. Angell was born in Canberra, Australia, and studied chemistry and metallurgy at the University of Melbourne. After working on molten salts with J. O'M Bockris at the University of Pennsylvania for two years, he became the Stanley Elmore Fellow at Imperial College of Science, London, where he completed his Ph.D. under the direction of John W. Tomlinson. There he was awarded the Armstrong medal for graduate research 1959−1961. He returned to Australia as lecturer in chemical metallurgy but after two years came back to the U.S. as a post-doc with Dieter Gruen at Argonne National Laboratory. In 1966, he joined Purdue University as Assistant Professor, becoming full Professor in 1971. In 1989, he moved to Arizona State University where he is now Regents' Professor of Chemistry and Biochemistry. He has enjoyed and profited from sabbatical leaves at the University of Amsterdam, the Australian National University, Institute Laue-Langevin, Grenoble, the Ecole de Physique et Chemie Industrielle, Paris, University of Rennes-Beaulieu, Sydney University, and the University of Rome. His research interests range from rechargeable lithium batteries and fuel cells, through the phenomenology of the glass transition and the origin of fragility in liquids, to the anomalous properties of water and geochemical fluids and their relation to polyamorphism. Currently, he is focusing on the annealing behavior of hyperquenched liquids and solutions, particularly denatured protein solutions, with a sideline on nanoporous network glasses as gas storage media.

I. What Is the Glass Transition? What Is the Fragility of a Liquid?

In a review of the present title, the first requirement is to ensure that the title words are understood. While the term "glass" is broadly familiar, and the origin of the "glass transition" in terms of the crossing of system and experimental time scales is generally agreed upon, there are at least three different definitions of the material property "glass transition temperature" (T_g) in current use.[1,2] Furthermore, these may differ from each other by as much as 50 K in certain higher T_g cases. The difference is a consequence of the magnitude of the "glass transformation range" within which the T_g is variously defined. This magnitude, the "width of the glass transition", can vary greatly from system to system, for reasons discussed below. Since the quantity T_g will recur frequently in this review, it is necessary to deal adequately with the definition problem, and this will be done by reference to Figures 1 and 2 below.

Depending on the liquid in question, glass transitions may be observed occurring over an enormous range in temperature, from below 50 K to above 1500 K. The reason for this range is clearly to do with the strength of the interparticle interactions, i.e., the "bonds" that are being broken as the particles rearrange. However, the reason that some glass transitions are "sharp" (meaning narrow glass transformation range, or "transition width") and others very spread out in temperature is not so clear. It is largely to do with the "fragility" of the glassformer, but may

10.1021/cr000689q CCC: $39.75
Published on Web 07/30/2002

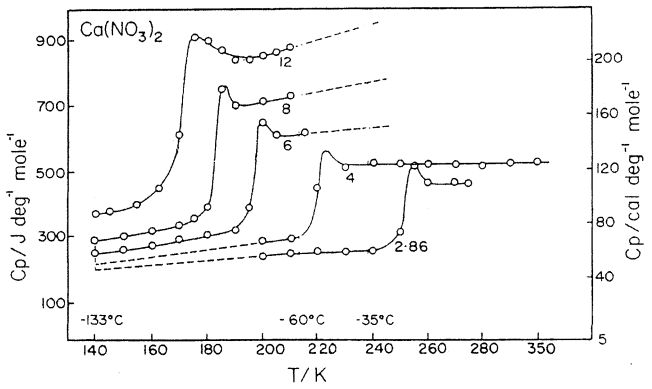

Figure 1. The heat capacity per mole of aqueous solutions of $Ca(NO_3)_2 \cdot RH_2O$ with R values from 3 to 15, where R is the ratio of water to salt in the composition under study. Note the increases in C_p that occur when the liquidlike degrees of freedom are liberated above T_g. One mole of water is seen to add an average of 10 cal/K to the jump in heat capacity at the glass transition in this system. The heat capacity jumps at T_g can he used to obtain data for a plot of the molar heat jump at T_g in relation to composition. By plotting against $1/R$, the heat capacity jump at T_g for pure water can be obtained by extrapolation. The value is greater than that observed[8,9] by a factor of 10, see below.

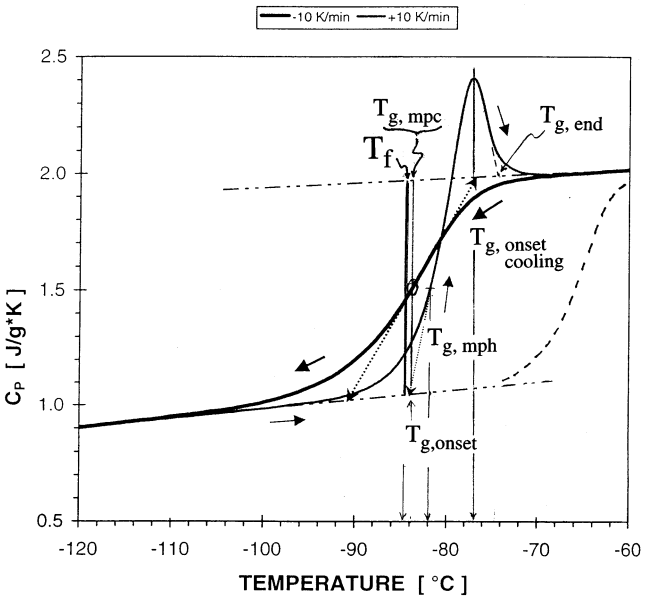

Figure 2. The calorimetric glass transition for glycerol according to differential scanning calorimetry during both heating and cooling. The different definitions of the glass transition that are currently in use are illustrated. The heavy vertical line shows the fictive temperature T_f, according to ref 27, and it is seen to coincide with the midpoint cooling definition $T_{g,mpc}$ and the onset heating glass transition $T_{g,onset}$. The midpoint heating definition, $T_{g,mph}$ falls at a higher temperature, as does the onset cooling definition $T_{g,onset\ cooling}$. The latter turns out to correspond to the overshoot peak temperature. The fictive temperature determined from cooling coincides with that from heating as a condition for accepting the cooling temperature calibration.[26] We emphasize that only cooling definitions are guaranteed to have no history dependence beyond that fixed by the cooling rate. The 10 Hz ac heat capacity curve, which is independent of cooling or heating rates in the vicinity of 10 K/min, is also shown (dashed curve). The curve obtained using temperature-modulated DSC would be the same as this if a modulation frequency of 10 Hz were instrumentally possible. Practical TMDSC contains aspects of both phenomenologies and records the overshoot of Figure 2 as a "non-reversing" heat flow. The width of the glass transition for glycerol, taken from the heating curve, is 9 K, giving a reduced width $\Delta T_g/T_{g,onset} = 0.047$, where ΔT_g is defined by $T_{g,end} - T_{g,onset}$. For non-fragile liquids, the reduced width is dominated by the fragility of the liquid (see section III).

also be influenced by the other characteristics of relaxing systems (nonexponentiality and nonlinearity) discussed below. The meaning of the term "fragility", which is of much more recent origin,[3] is less well established and the reason some systems are fragile, while others are not, is not at all well understood at this time.

The fragility is defined in terms of the deviation of the relaxation time temperature dependence from simple Arrhenius behavior. This deviation determines the steepness of the Arrhenius plot near T_g, hence the "sharpness" of the glass transition referred to above. It is generally recognized not only as a way of classifying glassforming liquids, but as a property that is predictive of both the nonexponentiality of the response functions and the extent to which they depend on the thermodynamic state of the system (the so-called nonlinearity of the response function). However, the best ways of quantifying the fragility are still being worked out. An additional problem with "fragility" is that it seems to have both kinetic and thermodynamic aspects, and an understanding of the relation between the two is in its infancy.

Among glass transitions, those that occur in concentrated aqueous solutions should be the most familiar of all since they have been under observation since time immemorial (vitreous sugar solutions, for instance, casein glues and gum tree resins). As will be seen in section III, some concentrated aqueous solutions are among the best characterized systems in the field. By contrast, the glass transition in water itself is mired in controversy[4−14] and, in our view, has never been observed.[14] We will devote the first part of this review to the characterization of the glass transition phenomenon in aqueous systems and the search for its existence in the case of water. The problem of explaining the term "fragility" more satisfactorily, and then quantifying and interpreting it, will be dealt with at the beginning of the second part.

II. The Glass Transition in Aqueous Solutions, and in Water

(a) Glasses from Aqueous Solutions

(i) Electrolyte Solutions

If a sample of "water" from the Dead Sea[15] (as a naturally occurring example of a borderline glass-forming salt solution) is placed in a small test tube, and the tube is plunged into liquid nitrogen, the liquid viscosity will be observed to increase continuously, without ice formation. After a few seconds, the liquid along the tube walls will become sticky and finally glassy. The warmer liquid in the center will then be pulled down as the remaining liquid continues to contract, and a "pipe cavity" will form. The half-hollow tube of saline water thus formed will become completely solid as the temperature of the

slower-cooling liquid at the tube center reaches the glass temperature, and the gravity-defying shape "freezes-in". Although the liquid has taken "taken the shape of its container" it can no longer fill it nor flow; hence, it is no longer a liquid according to the common understanding of the term. Finally, with continuing cooling, there will be an audible crack and the initially clear glassy mass will be observed to have become opaque. To the unaccustomed eye, it will appear that the glass has crystallized. However, what has actually happened is that the stress developed at the junction of the two glasses of different expansion coefficients (test tube glass and saline water glass) has exceeded the tensile limit of the saline glass and, in failure, the saline glass has abruptly developed a myriad of cracks.[223]

The whole process is reversed on reheating except that, as the glass starts to soften, a host of tiny ice crystals will usually form. When the composition is close to the limit of the "glassforming concentration range", the ice can start to crystallize while the glass is barely able to flow. This process should not be observed with unprotected eyes. The sudden expansion (due to the large volume of ice relative to the partial molar volume of water in the solution) without compensating flow can result in an explosion in which splinters of the test tube can be ejected quite dangerously.

These phenomena all occur because in the typical glassformer, which we will later see is a fairly fragile liquid, the flow properties change with extreme rapidity in a narrow range of temperature near the vitrification temperature.[16−19] A mere 10 K of temperature change can cause the viscosity to change by 3 orders of magnitude (which translates to an apparent activation energy many times the energy of vaporization). This means that, if a property under study can be measured with an accuracy of 1%, then its value will be observed to change from that typical of a liquid to that of a solid over a temperature interval of just 10 K. Such a sudden change warrants, in the eyes of most observers, the description of "transition", though the phenomenon is entirely kinetic in nature. Its position in temperature can be shifted dramatically by changing the time scale of the observation. Indeed, this is the only reason that water can ever be obtained in the vitreous state by cooling of the liquid. However, this interesting matter will only be discussed after an appropriate background has been provided.

The glass transition is usually characterized by the change in heat capacity which occurs as the state of equilibrium is reestablished during warming after an initial cooling into the glassy state at a rate sufficiently high that no crystals have formed. Examples are shown in Figure 1[20] for several solutions of different concentrations in the well-studied system calcium nitrate + water.[20−25] To deal with the different ways of quantifying T_g for a given glassformer, we use Figure 2 for the case of glycerol. The transition in glycerol is broader than in most molecular liquids. The various possible definitions[26] are collected in the figure caption. Three rather distinct definitions prove to coincide in value. These are the heating onset value $T_{g,onset}$, the fictive temperature, T_f,[16,27] and the midpoint cooling temperature $T_{g,mpc}$, the latter depending only on the cooling rate. All values used in this paper correspond to this unifying definition, for a cooling/heating rate of 10 K/min.

A "good" glassformer is one for which the cooling rate needed to avoid crystal formation is low. By this criterion, the majority of aqueous solutions of multivalent cation salts, and of most lithium salts, are good glassformers—when prepared above a critical concentration. The critical concentration depends mostly on the cation charge.[24] From an academic viewpoint, the failure to crystallize makes these solutions interesting because their transport properties can then be studied over the enormous 15 order of magnitude range typical of particle mobility changes between melting and glass transition temperatures in glassforming liquids. The system $LiCl-H_2O$, in particular, has been used as a model system in a number of fundamental liquid state studies focused on liquid dynamics,[28,29,31,32] crystallization kinetics,[33,34] and phase transitions,[35] about which much more will be said in section III of this paper.

Although the glassforming properties of aqueous solutions were well-known to the early German school of glass studies,[36] the first systematic study of aqueous salt solutions as glassforming systems was made by Vuillard.[37] It was in Vuillard's study that the best characterized case of a system ($H_2Cr_2O_7$ + H_2O) in which the glass cannot crystallize (because the unsaturated solution near the eutectic temperature is, at T_g, the thermodynamically stable state) was reported. Vuillard's study was extended by Angell and Sare[24] to include some 50 binary systems, and the relation between glassforming range and electrostatic charge concentration in equivalents/liter was established. The systems with trivalent cations were found to be capable of destroying the water-like arrangement of molecules needed for ice crystallization at concentrations as low as 3 mol % at ambient pressure. This study, and a later one concentrated on sodium salt solutions,[38] also demonstrated the strong effect of the anion basicity on the value of T_g for a given equivalent concentration. The more basic the anion (hence the stronger the hydrogen bond between water and anion), the higher the value of T_g. This relation has been turned to advantage in currently developing drug delivery and preservation systems.[40] It is found that citrate salts are the most effective because their higher T_g values lead to higher resistance to crystallization at the same concentration.

Interesting behavior is found in solutions of salts in which the cation is organic in character.[40] Here the ability of water molecules to form clathrate structures around the hydrocarbon side chains leads to highly cation-dependent properties.

(ii) Nonelectrolyte Solutions

While inorganic salt solutions have been well characterized by the foregoing studies, they by no means dominate the field of aqueous solution glasses. Many molecular liquids that mix exothermically with water will yield glassforming compositions, particu-

larly if the second component is glassforming itself. The two liquids most similar in properties to water itself, H_2O_2 and N_2H_4, yield easily glassforming solutions in the composition ranges 25−35 mol % of the second component,[41,42] but hydrates crystallize rapidly at higher solute contents.[42,43] On the other hand, solutions with the noncrystallizing poly-ol compounds propylene glycol and glycerol, are glass-forming at moderate cooling rates over all of the composition range above some 20 mol % of additional -OH group.[44−47]

Continuing this trend, aqueous sugar solutions are strongly glassforming. The only reason that sucrose is used for household sweetening is that the sweeter and cheaper sugar fructose cannot be crystallized from its aqueous solutions.[48] Several sugars, but most prominently the high T_g sugar trehalose, are used by nature to provide protection for spores, and indeed entire organisms, against death by dessiccation in dry times.[49,50] The sugars replace the water in the cellular structure and the immobile glassy shield protects the organism until the next rains arrive. Trehalose is currently finding increasing application in the food preservation industry since a cheap biosynthesis route was developed, and other sugars are being increasingly used to extend the shelf lives of pharmaceutical products. The region of composition in which T_g falls above room temperature for the sugars, sucrose and trehalose, is seen in the nonequilibrium phase diagram adapted from Schalaev and Franks[48] and shown here as Figure 3. Additional material on the applications of glass-forming propensity for cryo-, baro-, and anhydro- protection of bio- and pharmaceutical materials, will be included in the next section.

The variation of the glass transition temperature with solution composition for a wide range of systems is of interest. The data are displayed using a mol % composition scale, in Figure 4. The convergence of all plots to a common (extrapolated) temperature for pure water is one of the main reasons that the glass transition temperature for water is generally believed to lie at about 135−140 K. The first extrapolations indicating this as the T_g for water were given by Ghormley,[42] Yannas,[51] and Rasmussen and McKenzie.[52] We will later show that this is a dangerous extrapolation and that the assignment of 136 K as the glass transition temperature for water is in all probability incorrect.

(iii) Solution Glasses Formed Using the Pressure Variable

When pressure is introduced as a variable, the glass-forming propensity of all aqueous systems increases. This is because the nucleation temperatures of ice I_h are greatly lowered by increase of pressure as ice I_h is destabilized with respect to the liquid state. The nucleation probability lowering for ice I_h continues without limit, but above about 200 MPa the nucleation of ice III becomes equally probable and, thereafter, more probable, and so the increasing tendency toward vitrification is arrested. At this pressure, where the melting point has been maximally lowered (to −23 °C), the homogeneous nucleation temperature (determined using emulsion

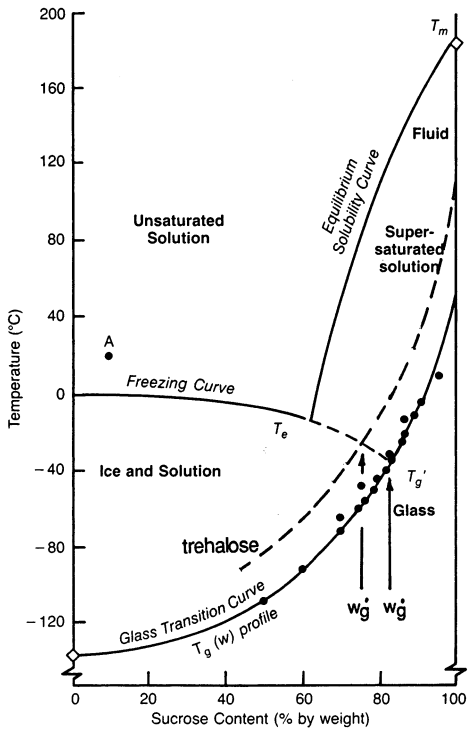

Figure 3. Phase diagram for the system water + sucrose, showing the equilibrium liquidus lines and the metastable extensions manifested under common cooling conditions. When the nucleation of ice from the metastable supersaturated solution becomes too slow, then glasses form on further cooling. The glass transition temperatures for sucrose water solutions are shown over the range in which ice-free glasses can be obtained and the conventional extrapolation to the temperature −134 °C for water is made. The heavy dashed curve shows the corresponding higher temperature plot for the disaccharide trehalose (Adapted from ref 48 with permission. Copyright 1995 Elsevier).

samples) has been reduced to −92 °C,[53] and the water has a viscosity like honey. Indeed, small samples of pressurized pure water can now be vitrified at cooling rates that are not too difficult to achieve.[55] The author once observed a 2-cm length of water held in a strengthened glass capillary tube, 10 μm in diameter, at 1950 MPa by oil pressure, remain unchanged in length on plunging into liquid nitrogen (ice I formation causes length to increase) but was unable to repeat the observation. Like glycerol,[54] water can evidently impress its crystal structure on the physical surroundings and, once crystallized, can always find the route a second time. On the other hand, Mishima[55] has now reported that pure water, in emulsified form, can be vitrified reliably by cooling at fast (but not hyperfast) rates, $Q > 10^3$ K/s. This will be further discussed in section IIb below.

Addition of second components will of course provide a different source of liquid stabilization that adds on to the pressure effect, because salts and other molecular components are quite insoluble in the ice lattices. The melting point lowering effect then decreases the nucleation temperature until it falls below T_g and the glass-forming region commences. Under 200 MPa pressure, almost all aqueous solutions have glass-forming regions. NaCl solutions, for instance, never vitrify at normal pressure under

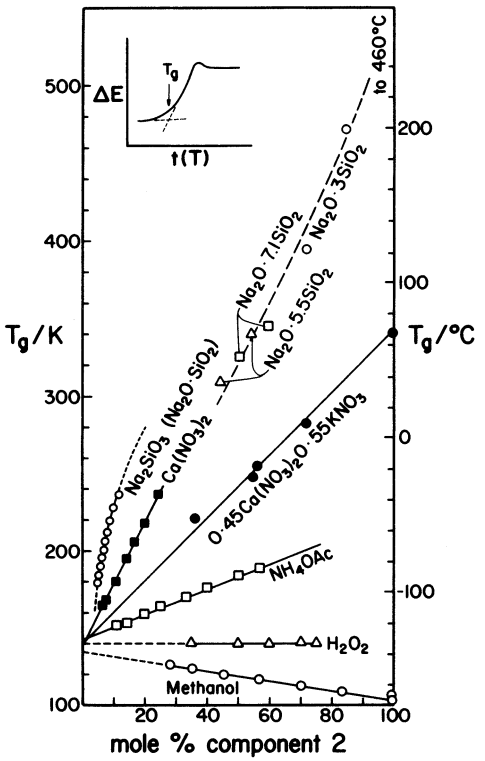

Figure 4. Variation of the glass transition temperature with composition for various binary solutions of which water is the common component. The natural extrapolations indicate that water should have a glass transition temperature of about 135−140 K. However, such natural extrapolations may be misleading in the case of systems where one component is a network-former, as will be documented later (Reprinted from ref 7 with permission. Copyright 1984 American Chemical Society).

normal cooling procedures. However, above 200 MPa they become glassforming in bulk in a narrow composition range, $R = 12-16$ (R is the mole ratio of water to cations) and are glass-forming with as little as one Na^+ ion per 20 molecules of water ($R = 20$) when in emulsion form.[56] The glasses formed under high-pressure often give a peculiar thermogram during warm-up, showing what appears to be a second glasslike endotherm at temperatures higher than those of the primary glass transition.[56] The primary glass transition is found near −120 °C and, like the value of T_h above 200 MPa, is only weakly dependent on pressure. The second endotherm, seen at 150 K and above in isobaric experiments, has been described in more detail by Kanno[36,57] and interpreted as the glass transition temperature of a distinct phase, which is deduced to be due to a water-rich phase. This will be discussed further in section IIb below.

At pressures above 200 MPa, trivalent cation salt solutions can be vitrified in bulk with only one cation for 60 water molecules.[56] This could fall to one cation for 100 waters, for solutions in emulsion form. No reports are available for cations such as Zr^{4+} and Th^{4+} whose salts in water have large glassforming regions.[37,38]

The pressure dependence of the homogeneous nucleation temperature has also been studied in solutions of hydrophilic molecular liquids because of the interest in using such solutions to suffuse human tissue, and thus, by suppressing ice nucleation during cooling, assist in the cryopreservation of blood, sperm, and even whole organs.[58,59] A separate interest has been in providing hydrous media, in which ice does not crystallize during cooling, for the high-resolution electron microscopy of plant and animal cells.[60]

For cryopreservation purposes, detailed studies of the systems propane diol + water and dimethyl sulfoxide + water, neither of which is toxic in moderate concentrations, were carried out by Boutron and co-workers,[61] but the concentrations needed to prevent crystallization of ice were high enough to enter the toxic range. Presumably this is because biological function and crystallization both have need of water in a state capable of maintaining open tetrahedral networks at least in "patches". The possibility of substituting pressure for part of the second component, and thus avoiding the toxic range has been the motivating force behind studies by Fahy[58,62] and MacFarlane.[63]

Recent studies on cryopreservation technologies have concentrated on more effective solutes including racemic mixtures[64] rather than on pressure. Sugars, in particular the disaccharide trehalose mentioned earlier,[49,50] have been given a lot of attention[65−68] partly because of their strong effect on the glass transition temperature,[50] which however is certainly not the only factor involved.[66−69] These systems tend to be used in high concentration because they are of low toxicity and the sugar can, by hypothesis, replace water in the cell structure without causing damage.[66] In some cases, a polymeric glassforming additive is found advantageous, e.g., hydroxyethyl starch, for blood preservation.[70] This application of glass transition phenomenology, with and without the help of pressure, continues to attract much attention.[71−73]

(iv) Solution Glasses Formed by Nonliquid Routes

It might be supposed that aqueous glasses are always formed by cooling (or compressing or drying) a *liquid* or *liquid solution*, but Suga et al.[74] have shown that this is not the only way to obtain aquated glassy phases. These workers demonstrated the formation of an aqueous magnesium acetate glass by partial dehydration of the crystal. The same was later found to happen with the sugar hydrates raffinose pentahydrate[75] and trehalose dihydrate.[76] This process depends on the destabilization of a crystal phase by partial removal of one of the lattice components.

In its dependence on a lattice destabilization, the latter process is related to another nonliquid route which is of great relevance to the case of water itself. This is the pressure-induced amorphization route which is of general interest to glass science but which was pioneered by Mishima[77,78] for the case of pure water (see section IIb). The compression method yields the higher density member of two polyamorphic forms of water, which will be discussed in the next section. Water has also been vitrified at low temperatures by depressurizing a high-temperature stable crystalline state, ice VIII.[79] This route yields the lower density polyamorph. It is reasonable to expect the decompression-amorphization route to be more applicable to the generation of aqueous solution

glasses than the compression route, which depends on an uncommon initial open-packed structure. No examples of such decompression amorphization processes for solution glasses are yet available, though their structural relation to the "normal route" solution glasses discussed above would be interesting. Candidate materials would be high pressure forms of high hydrates such as $MgCl_2 \cdot 12H_2O$.

(v) Relation of Glass Transition to Liquid Properties

Since it is the end point of the liquid state during cooling (or pressurization, or desolvation), the glass transition occupies a singular starting point for consideration of liquid state behavior, namely, the "solid state approach" to understanding liquids.[2c] In any such approach, it must be borne in mind that the glass transition is only a kinetically imposed limit on an underlying *equilibrium* physics of excited amorphous solids. It is in this underlying equilibrium physics that the challenge to theory offered by this approach lies.

The liquid state properties of this wide variety of glass-forming systems, and the manner in which they are influenced by, or reflect, the underlying glass transition, will be considered in section III. Before leaving the present section, however, the rich history and science of the glassy state of pure water, and in particular, of the effort to assign it a glass transition temperature, must be considered. It is one of the more interesting stories of science history, and the manner in which the behavior of this simple molecule in its condensed phases has deceived all its investigators is worth spending some time to describe. Thus, we deliberately choose a narrative form for the next section.

(b) Glassy Water

While liquid water is the most abundant form of water on earth, our world is an anomaly in the universe. The H_2O molecule, on the other hand, is ubiquitous. It occurs most abundantly in amorphous films on tiny grains of solid material scattered throughout the vastness of space. Where unusual opportunities for accretion exist, the grains will form large bodies. We witness these in the periodic visitations of comets. The major component of the typical comet is water, and the form of the water, according to the best information available, is amorphous.[80] Since planets are presumed to be scarce, glassy water is probably the most abundant form of water in the universe.

This vapor-deposited material, as it is studied in the laboratory, has been called amorphous solid water ASW,[81] and it has been the subject of study since 1935 when Burton and Oliver[82] first demonstrated that it was amorphous by X-ray studies. Since it has the appearance of a glass when carefully prepared, it has been natural to enquire after the value of its glass transition temperature. It is the fluctuating and still uncertain answer to this question, over 50 years of controversy, that is the focus of this section. We will deal first with the subject of the glass transition in this material and its close relatives. We will then consider the equally intriguing questions of the glassiness and glass transition temperature of the polyamorphic high density form of glassy water made by the pressure-induction method and, very recently, by high-pressure quenching of emulsion samples.[55] It is quite likely that this form has been made, but not recognized, much earlier, in the "slam-quench" preparation of samples for high quality electron micrographs of plant and animal cells, developed by Heide and Zeitler.[83] The apparatus of these workers was designed to instantly raise the pressure on a thin sample of a cell suspension to values of order 200 MPa during cooling to 77 K, using colliding 77 K plates. The authors reported that the electron microscope images of samples prepared by this technique established the absence of any crystalline structures in the 77 K products of the quench process.

(i) The Glass Transition Temperature of ASW, and Its Relatives

The subject of the glass transition temperature of the amorphous solid form of water has a checkered history. Pryde and Jones[84] were the first to deliberately seek to establish its value, and they were disappointed by their failure to find any way of assigning it. The usual thermal signature, illustrated in Figure 1, was not found within the precision of their experiment (except for one initial and irreproducible experiment). Like everyone since, they expected to find the glass transition in the vicinity of 140 K because of a Vogel Fulcher equation extrapolation of the existing liquid viscosity data.[84] Ghormley, who performed several characterizing experiments on the vapor-deposited solid,[6] also failed to find a thermal effect, though he obtained values of the heat of crystallization that are quite close to the presently accepted value of 1.29 J mol^{-1} K^{-1}.[10,85]

Shortly thereafter, MacMillan and Los[5] prepared glassy water by direct deposit onto the pan of their vacuum-mounted differential thermal analysis apparatus, and observed a well-defined endotherm at 139 K. This was apparently confirmed by the subsequent study of Sugasaki et al.,[4] who deposited ASW in an adiabatic calorimetry cell and repeatedly observed an endothermic effect which, unfortunately, was never completed before crystallization of the sample occurred.

Olander and Rice[86] refined the deposition process, and the transmission IR spectra they recorded suggested that crystallization of the glasslike deposit never occurred below ~160 K. This was confirmed in subsequent studies from Rice's group.[81] Encouraged by the increased temperature range apparently available, Macfarlane and Angell[3] carried out the deposition according to Olander and Rice's prescription, directly into a DSC pan, so that precise quantitative measurements of the heat capacity jump could be made. However, after an initial positive result at the expected temperature was traced to vacuum pump oil being used to provide a thermal connection to the DSC pan, they were unable to detect any thermal effect at all before crystallization occurred. The sensitivity of the measurement was much greater than needed to detect either the jump

reported in ref 4, or the smaller jump anticipated from solution data extrapolations,[20] e.g., using data from Figure 1. Accordingly, MacFarlane and Angell concluded that the glass temperature lay above the crystallization threshold, as known to be the case for many hyperquenched metallic glasses, hence could not be observed.

Then, Bruegeller and Mayer[87] and Dubochet and McDowell[88] almost simultaneously reported the preparation of glassy water by rapid quenching of microscopic samples of water into a cryogenic liquid. Bruegeller and Mayer identified the formation of a glassy state by the subsequent release of the heat of crystallization of the quenched substance, though again no actual glass transition was detected. Dubochet and McDowell detected it by the diffuse diffraction rings in electron microscope studies. Mayer and co-workers[89] subsequently determined that the glassy phase obtained in this manner was likely to be contaminated by inclusion of molecules of the cryoquench liquid in the vitreous water network. To avoid this, Mayer[90] developed the aerosol droplet hyperquench method in which hypersonic droplets formed by vacuum expansion, were splatted against a liquid nitrogen-cooled substrate. This conglomerate of tiny quenched droplets, called HQG water, could then be studied microscopically, spectroscopically,[91] or calorimetrically[8,92−94] as desired. (Alternative droplet vitrification methods for water have recently been reported.[224])

Because of its manner of preparation, the aerosol-derived glassy water is probably as pure as it is possible to obtain (however, see ref 224). Subsequent studies of the conglomerate[8,92] showed that, after sufficient annealing at temperatures near 120 K, it yielded a weak and spread-out DSC endotherm commencing at about 136 K. This was assigned to the glass transition temperature for vitreous water. A similar behavior was then observed, and interpreted as a glass transition, for ASW.[95] A summary of these endothermic effects obtained for ASW) is shown in Figure 5. A similar phenomenon occurring at a slightly lower temperature, and looking even more like a glass transition, is also seen[96−98] for the analogue material obtained by the pressure-amorphization route,[77,78] and called LDA (for low-density amorphous water, discussed below). The change in DSC output expected at a T_g of 136 K from an extrapolation of the heat capacity change per mole H_2O in the solutions of Figure 1, is also shown by the arrow to the right of the figure, and the discrepancy is obvious.

Although this value of 136 K for the T_g (onset value) of water, based on Figures 3, 4, and 5, has been widely accepted by the scientific community, there are reasons to be concerned about it. The first is that glasses that can only be formed by use of extreme quenching rates, usually do not exhibit a glass transition on reheating. The reason is that in such cases the rate of relaxation into the crystalline state is usually higher than the rate of relaxation to the very low enthalpy states found near the normal glass transition. In this case, the crystal forms (nucleates and grows, with the release of the crystallization

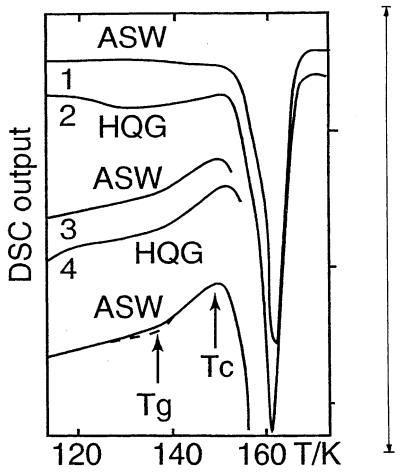

Figure 5. Calorimetric effects on as-formed, and annealed, samples of amorphous waters used as bases for assigning the glass transitions for these materials. ASW (curve 3) is the vapor-deposited form, HQGW (curve 4) is the hyperquenched liquid form, after annealing while curves 1 and 2 are for the as-prepared materials. T_c is the crystallization temperature. The vertical arrow on the right-hand side indicates the jump in heat flow at the temperature of 136 K expected for water by extrapolation vs $1/R$ of the data in Figure 1. (This requires comparison with heat capacity values deduced for ASW and HQG water in ref 9, with the ΔC_p values deduced[95] from these DSC heat flow curves). The failure of the extrapolation is striking. To understand these endotherms properly, see Note Added in Proof. (Adapted from ref 95 with permission. Copyright 1989 American Chemical Society).

enthalpy), before the upswing in C_p characterizing the glass transition can commence. (The early stages of annealing, which occur much more rapidly than nucleation because they occur on shorter length scales, take place entirely in the amorphous state).

The question then arises, why should the glass transition remain detectable in the case of water, if indeed the 136 K phenomenon is the glass transition? The natural answer is that water is odd in every other respect so why not this one. The problem, however, runs deeper than this facile answer can satisfy. There is a fundamental conflict of the enthalpy recovery of hyperquenched water during upscan[93] with what is well-known about relaxation of enthalpy near the glass transition. The problem can be described as follows.

The enthalpy relaxation time at the glass transition (obtained by repeated analyses of the glass transition endotherm,[16,99−100] and confirmed by many parallel dielectric relaxation time studies[101,102]) is 100−300 s. This means that, in one relaxation time, a fraction $1 - e$ (or about 2/3) of any displacement of the enthalpy from its equilibrium state will be relaxed out. If the perturbation is large the relaxation rate will be larger at the same temperature. In a number of cases where hyperquenched glasses have been studied,[14,103,104] it is seen that *all* of the large frozen-in enthalpy is relaxed out (and the system has recovered its normal equilibrium state) by the time it arrives, during an upscan, at a temperature of $1.1T_g$, i.e., by the end of the glass transformation range. This complete recovery temperature would be $1.07\ T_g$ for glycerol (see Figure 2) or $1.04T_g$ if the

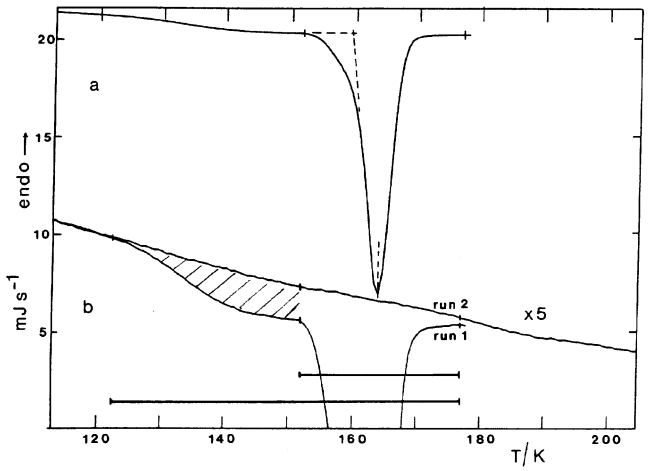

Figure 6. (a and b) Initial, and second, differential scanning calorimeter upscans of hyperquenched glassy water, showing (hatched area in b) the exothermic release of enthalpy stored in the hyperquenched state. Because all the amorphous material has converted to cubic ice above 170 K the rescan shows only the heat capacity of cubic ice and provides a suitable background scan to assess the "excess heat capacity" provided by the enthalpy relaxation process, which is obviously incomplete when crystallization takes over (Adapted from ref 93 with permission. Copyright 1987 American Chemical Society, and from ref 14 with permission from Science (http://aaas.org). Copyright 2001 American Association for the Advancement of Science.). Part a shows the data at lower sensitivity such that the entire crystallization can be seen.

liquid is fragile, like *o*-terphenyl). Here, as before, T_g is taken to be the temperature of the onset of the heat capacity "jump" during a heating upscan at 10 K/min (Figure 2). The examples under consideration include both fragile and strong glassformers.[103] This "complete recovery" temperature would correspond to 149 K in the case of water if its T_g is 136 K and if it is a strong liquid. If it is considered to be fragile[13] then the complete recovery temperature would be 142 K. Why then, we have to ask, is the excess enthalpy of hyperquenched vitreous water still largely unrelaxed at 150 K when it starts to crystallize, as shown by the careful study of Hallbrucker and Meyer,[93] and reproduced in Figure 6.

Figure 6a compares the upscan of the as-quenched glass with a baseline established by the rescan after crystallization, which is enthalpically neutral. It is clear, from the difference in the two scans at 150 K, that the relaxation time for much of the frozen-in enthalpy is much longer than 200 s at 136 K. Even at 150 K much of the excess enthalpy trapped in the glass during the hyperquench remains unrelaxed. Mayer [private communication] has kindly shared unpublished data on many other hyperquenched water rescans with the author and they all show the same qualitative behavior, though some, from slower hyperquenches, appear to be further through the excess enthalpy relaxation process than others at the crystallization temperature.

This argument has been presented in more detail elsewhere,[14] and will not be repeated here. It leads to the conclusion that either there is some new phenomenon, possibly associated with quenched-in, intrinsically slow, critical fluctuations,[14] or else the glass transition temperature for water is not 136 K but some higher number that is not directly measurable because of pre-emptive crystallization. It is basically fatuous to speculate on the value of a quantity that cannot be observed unless some related behavior can be explained in terms of such a value, as in the case of "hidden" critical points, for instance. Here a T_g assignment is useful because of the relevance to the early annealing behavior of HQG water. The early annealing behavior can be rationalized by using a revised value of T_g for water (a hidden T_g) of ~165 K.[14,103] See Note Added in Proof concerning the revised value of T_g.

The above constitutes a significant revision of the value of T_g ascribed to water and a return to the earlier conclusion of ref 3. However, it has several advantages. It permits one to understand the previously puzzling finding by Johari and co-workers[98] that different amorphous waters do not relax to the same material when held for various times at or above the (previous) T_g. This led them to postulate the existence of different forms of liquid water, water A and water B, which cannot interconvert. It also permits one to understand the failure of water films, containing electron sources and studied after irradiation, to show the isotopic scrambling expected if the diffusion coefficient were that of a liquid.[11,105] It permits one to understand why the activation energy for the subsequent crystallization process (the kinetic constant in the Avrami equation for crystallization rate) should have such a low value (50−70 kJ/mol). Several quite independent research groups[106−108] have reported values in this range. It is a standard argument in the kinetics of phase transformations[109,110] that this activation energy should be close to that of the diffusion coefficient in the transforming medium—in the case of glassformers, also close to that of the viscosity. It is not surprising that this activation energy should also be in the range of the activation energy for diffusion in ice if the system is still in the glassy state when crystallizing. Previously,[111] we had used such data to argue, on the assumption that $T_g = 136$ K, that ASW and HQGW are extremely "strong" liquids. This is clearly no longer necessary. (However, see the final section of this paper for another ironical twist, an analysis in which we see that water must still behave as a strong liquid below about 210 K.[112] It will be seen there that the value of $T_g = 165$ K was actually predicted before it was deduced by the ref 103 analysis. In section III of this paper, we will see evidence of residual effects of this transition in the liquid-state behavior of glassforming solutions)

While the reassignment explains the above puzzles it apparently leaves unresolved why, in Johari's blunt probe dielectric measurement,[113] penetration of an ASW film was observed, while penetration of the corresponding crystallized film was not. However, later we will see evidence that, as with SiO_2, pressure anomalously decreases the T_g of LDA or ASW, hence, at the probe tip, flow may occur. This is related to the "cutting amorphization" phenomenon observed by Dubochet and co-workers in electron microscopy after microtoming, which is referred to below. Even with-

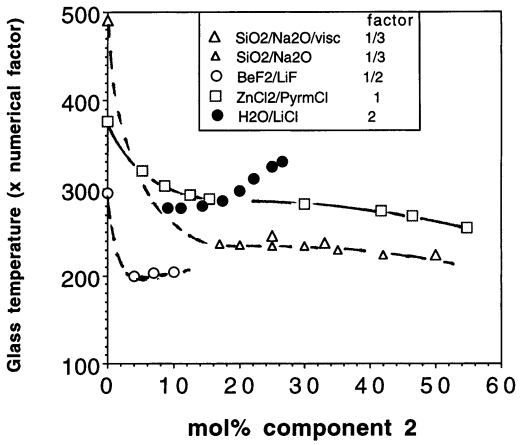

Figure 7. Glass transition temperatures for solutions containing tetrahedral network-former first components. To bring systems of very different glass temperatures together, temperatures for each system are scaled by the factor listed in the legend. Note the abrupt drop in T_g value as the network is disrupted by the second component and the plateau region following the initial drop.. The plateau region is seen for the $H_2O-LiCl$ system, but the rapid drop in T_g is hidden by crystallization, and hence remains a hypothesis. However, the hypothesis is strongly supported by the behavior of the "shadow T_g's" in binary aqueous solutions. See Note Added in Proof and ref 226.

out this effect, flow satisfying the criteria for liquid-like viscosity can be expected below T_g, according to studies on both fragile and nonfragile liquids (see Figure 21 in ref 224, and Figure 9 in ref 18). The T_g reassignment also leaves unexplained the at-first-sight-convincing extrapolation of the data in binary solutions, shown in Figure 4. However, in this latter case, there are data on analogue systems, shown here in Figure 7, that can provide a convincing resolution of the apparent problem.

Figure 7 shows the composition dependence of T_g in three systems whose key components, SiO_2, BeF_2, and $ZnCl_2$ share with water the much-referenced "tetrahedral network" structure. The tendency to achieve this structure, in competition with thermal disordering forces, is always cited as the reason for the density maximum in water, and as the explanation of other highly anomalous properties in the supercooled liquid state. The "random tetrahedral network" is established almost to perfection in the glassy state of water according to the X-ray studies of Venkatesh et al.[114] $ZnCl_2$, BeF_2, and SiO_2, the latter two of which also show a density maxima,[115−118] are all systems in which crystallization does not prevent the direct observation of the glass transition. Thus, in these cases, unlike that of water, the glass transition temperatures in binary systems can be measured continuously as the pure component composition is approached. Network former-based binaries resemble each other because cold networks, that are naturally low in configurational entropy, rapidly gain it on mixing with network breakers. Accordingly, they rapidly change viscosity (and glass temperature) with initial additions of network breaker. However, the products of the network breaking are not well miscible with the network so a domain of immiscibility, or tendency thereto, follows. This is well-known in the case of silicate glasses, and sub-liquidus liquid−

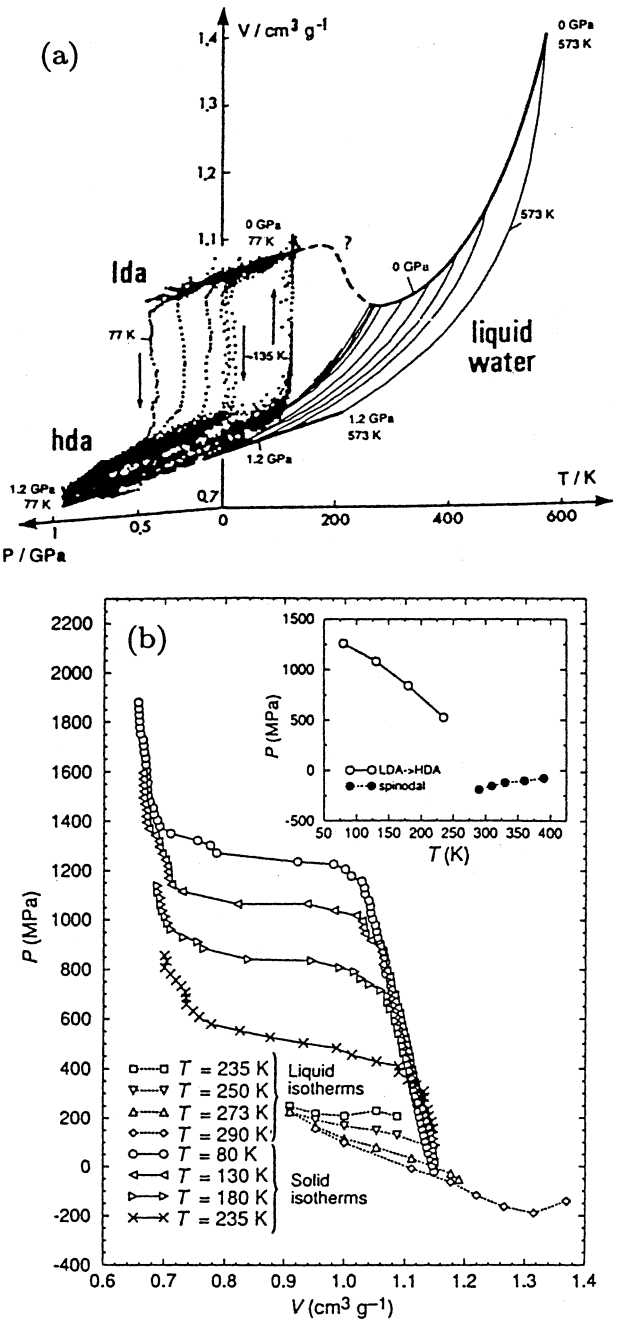

Figure 8. (a) Cycling between high and low density forms of amorphous water HDA and LDA at different temperatures, from Mishima[78] and (b) the equivalent P−V relations, for different isotherms, from the molecular dynamics study of Poole et al.[123] using the ST2 pair potential.

liquid demixing in the system BeF_2-LiF has also been well documented by the electron microscopy studies of Vogel and Gerth.[118] However, the striking behavior of T_g, in BeF_2-rich glasses in the $BeF_2 + LiF$ system (included in Figure 8), had not been recorded until recently.[119] According to these authors, T_g for the solutions must increase some 200 K as the last 2 mol % of LiF is removed. The suggestion is that the behavior of the LiF-containing glass is dominated by quartz polymorph-like BeF_2 behavior, whereas pure BeF_2 is crystobalite polymorph-like, as indicated by its crystallization products. The quartz-like BeF_2 polyamorph has a much lower T_g than the open network crystobalite-like polyamorph. We might

expect similar differences for the polyamorphs of water, HDA, and LDA.

The rapid upswing in the values of T_g in the last 5 mol % of the network- forming-compound is the main feature of the three cases for which data are presented in Figure 7; however, the T_g plateau region associated with tendency to sub-liquidus unmixing is also notable. This plateau feature is also present in the $LiCl-H_2O$ system in the observable region, as shown by the data of Sare[24a] included in Figure 7. It seems very reasonable, in light of Figure 7, that there should be a similar T_g upswing on the case of water, were it not hidden by crystallization. The upswing in the viscosity of water-rich binary systems is very pronounced in the supercooled regime[120] as will be detailed in section III of this paper. Figure 7 certainly suggests that there is reason to be concerned about the validity of the extrapolations of Figure 4, which now appear to be quite misleading.

(ii) Polyamorphism: High and Low Density Glasses of Water

One of the most astonishing developments of the 1980s concerning the glassy state of matter was the report from Mishima and colleagues[77,78] that glasses could be generated directly from crystals by application of sufficient pressure, provided the temperature of compression is low enough (77 K in the case of ice I_h). Sciortino et al.[79] subsequently pointed out that this phenomenon had actually first been recorded in reverse, by the observation in 1975 of a glass formed in consequence of the decompression of a high-pressure stable perovskite silicate.[121] However, it was Mishima's discovery for the case of water that awakened interest in the subject. Since then, the vitrification of many materials by cold compression has been demonstrated,[122] though the "vitrification" is sometimes only apparent and is reversed on decompression.[122b]

The most remarkable feature of the dense glassy product of compression in the case of water is that it proves to be capable of being cycled in and out of the dense state. This is achieved by raising the temperature at ambient pressure to obtain a low-density amorphous material (LDA) and raising the pressure again at lower temperature to regenerate the high-density amorphous state (HDA).[78] The term "amorph" is used because the viscous liquid state was never clearly observed and the glass transition has been controversial. The observed behavior is reproduced in Figure 8a, and the similarity to the behavior generated by molecular dynamics MD computer simulation using the ST2 potential on a periodic box containing 500 molecules,[123] shown in Figure 8b, is obvious. Similar results are obtained with other reasonable pair potentials, e.g., TIP4P, TIP5P, and SPC-E.[124−125]

The simulation, unlike the experiment, is clearly dealing with a state that can be reached repeatedly by cycling the temperature up into the *liquid* and down again. Thus, the term "glass" is quite applicable, even if it is a glass generated by a quenching rate impossible to achieve in the laboratory. Unlike the case of Figure 5, the change in heat capacity on passing from liquid to glassy state is large,[125] though its value has not been featured in any discussion. This is partly because, in the simulation, ergodicity is broken at a temperature that is still in the viscous liquid state in the laboratory. It may also be because, in the *experiment*, the viscous liquid state is in fact not being accessed, as argued earlier in this review.

An alternative though related route to HDA seems to be what is called "cutting amorphization", in which the shear stress of the leading edge of a microtome blade causes the transformation.[126]

A question arises about the possibility of observing the glass transition on heating the high density amorph, given that the crystal nucleation temperature has been reduced so substantially under pressure. Because of this stabilization of the liquid, it could be hoped that the glass transition might become observable before crystallization. This is indeed a reasonable expectation for a liquid that can be vitrified at 10^3 K/min quench rates, given the successful observations of T_g in other emulsified liquids that are not normally glassforming.[127] However, even in emulsion form, in which ice I_h "melts" by spinodal collapse (i.e., by a one-phase rather than a two-phase process) at high pressure and $T < 150$ K, it seems that HDA crystallizes before it manifests a glass transition.[128]

Both the glasses formed by water using the pressure-induced amorphization route, HDA and LDA, seem to be very unusual.[129,130] They lack the usual Boson peak so common to the glassy state,[131] and LDA shows sharp resonances in inelastic neutron scattering at high wave vector[130] as if high Q phonons are well-defined excitations in this system. A proper explanation of these features is not in hand at the moment. It is possibly generic to tetrahedral glasses that lack large bridging units, because amorphous silicon shows some similar features.[132]

The special interest in the apparent polyamorphism for water lies in whether a critical point, at which the properties of the two amorphous phases would become identical, exists. Judging by the temperature dependence of the boundaries of the two phase region, seen in Figure 8 (which are spinodal rather that equilibrium boundaries since they are obtained by out-of-equilibrium measurements), the critical point would have to lie within the liquid region. Except for the case of SPC-E, the results of the computer simulations mentioned above indicate, with little question, that such a critical point exists. So also do the results of clever DTA studies of the metastable melting transitions for high-pressure ice polymorphs.[133−135] Such a singularity for water would provide a basis for unifying the treatment of all the anomalies in behavior of this most important of liquids, and a direction for treating anomalies in other related liquids. Its confirmation is therefore a matter of great importance.

The critical point would appear to lie just below the homogeneous nucleation temperature for ice I_h, indeed close enough for the critical fluctuations to have some influence on the observable properties well beyond the critical temperature and out into the metastable liquid range. Therefore, suitable scatter-

ing measurements on emulsified samples near the homogeneous nucleation temperature might be able to provide the evidence needed to convincingly demonstrate that this critical point exists. Of some concern in this respect is the finding that proton NMR measurements that penetrate to the homogeneous nucleation temperature seem to show monotonic variations of the relaxation time temperature dependence through this pressure range.[136,137] The best fit to the power laws expected for critical phenomena seem to be obtained at ambient pressures in these studies. Some assistance in clarifying the phenomenology in this fascinating region may become available through studies on analogue systems such as liquid Si, in simulations of which the existence of a metastable first order phase transition (rimmed by spinodals) states, occurs between two liquids in a computationally more accessible region.[138]

(iii) Vitreous Polymorphs by Demixing from Aqueous Solutions

Before leaving this section, we need briefly to consider an alternative means of producing glassy water which has only been mentioned in passing so far in this paper (in connection with Figure 7). This involves a process that has been discussed several times but is still not on firm ground.[35,38,57] It involves the separation of water from binary solutions at low temperatures by a liquid−liquid demixing route. This is the analogue of the process that generates almost pure glassy SiO_2 droplets from different multicomponent silicate systems of appropriate compositions, such as Na_2O-SiO_2 in the plateau region of Figure 7. Although this analogy was suggested long ago[38] as a possible means of explaining the behavior of glassy $LiCl-H_2O$ during solutions warm-up, and peculiarities in the glass transition endotherms of propylene glycol$-H_2O$ solutions near the boundary of the glassforming region,[139] it has not been confirmed by direct observations, e.g., electron microscopy. Light scattering evidence for its existence[140] was not confirmed by low angle neutron scattering studies.[141] Nevertheless, scanning calorimetry work by Elarby-Aouizerat et al.[33b] was interpreted as indicating two glasses transitions, slightly different in temperature, in certain composition ranges of the $LiCl-H_2O$ system.

While not observing anything to clearly justify two distinct glasses in studies of $LiCl-H_2O$ solutions at ambient pressures, Kanno[35] found, at higher pressures, that two quite distinct endothermic DTA effects are present. These became distinct in the pressure range in which the work of Mishima and Stanley[132,133] suggests that the low temperature phase of water becomes thermodynamically distinct from the high-temperature phase. Kanno associated the higher T_g with the water-rich component. By forming the glass at high pressures and observing its behavior at lower pressures, Kanno was able to observe the upper glass temperature approach the value of the lower one. This suggests that a high-density glassy water might, like the quartz-like polyamorph of BeF_2 discussed earlier,[119] have a lower value of T_g than the open network form. Thus, the possibility is raised of obtaining vitreous water in one or other polyamorph by low-temperature phase separation from the binary solution glass. By tuning the pressure in the manner of Mishima[78] (Figure 8a), it might be possible to demonstrate the separation of glasses of different density.

The above scenario is reminiscent of the manner in which another highly unstable glassy material has been observed to form. This is the case of spherical droplets of amorphous germanium seen (in electron microscopy) to separate from $Ge-GeO_2$ glasses by annealing at temperatures below the crystallization temperature, and also below the T_g, of the initial glass.[142]

Mishima has separately observed two distinct Raman spectra for Kanno's pressurized $LiCl-H_2O$ solutions.[143] These spectra are compatible with the suggestion of Kanno, although they were observed in hyperquenched samples. What is needed here, and for the propylene glycol solutions of ref 139, is the equivalent of the electron microscopy studies of ref 83 applied to the case of $LiCl-H_2O$ solutions.

Finally in this section we emphasize the phenomenological similarity of systems involving tetrahedral network systems by comparing phase diagrams for the cases such as those exhibited in Figure 7. In ref 38a, the phase diagrams for (i) H_2O + LiCl, (ii) Na_2O + SiO_2, and (iii) Ge + Se are shown together. There it can be seen how the well-characterized[109] submerged immiscibility dome in the SiO_2 + Na_2O system becomes a large thermodynamically stable immisciblity dome in the case of Ge + Se, or Si + S systems. Water + LiCl probably presents an intermediate case in which the immiscibility dome is submerged but because of rapid crystallization kinetics, unmixing to form the water-rich phase is immediately followed by crystallization. It is at the low-temperature edges of such zones that nanoscopic spheres of the second liquid phase might be observable by electron microscopy, as in the case of the Ge + GeO_2 glasses mentioned above.

III. Fragility of Aqueous Solutions and Water

(a) Liquid and Solution Fragility

The relation of the term "fragility" to the deviation of supercooled liquid relaxation processes from Arrhenius temperature dependences has been mentioned in the introduction. "Fragility" is a word that, in reference to liquids, attempts to capture the aspect of supercooled and viscous liquids between melting and glass transition temperatures that is the most provocative, from the standpoint of condensed matter physics. This is the large, and "super-Arrhenius", temperature dependence of the mass transport, or relaxational, properties that is usually to be observed. The viscosity of molecular liquids, for instance, can change by 3 orders of magnitude in an interval of 10 K near T_g. This translates to an apparent activation energy far greater than the energy of vaporization.[144] Such behavior is associated with a very unphysical value for the pre-exponent of the Arrhenius expression and is often attributed to the cooperative nature of the relaxation process in supercooled liquids.

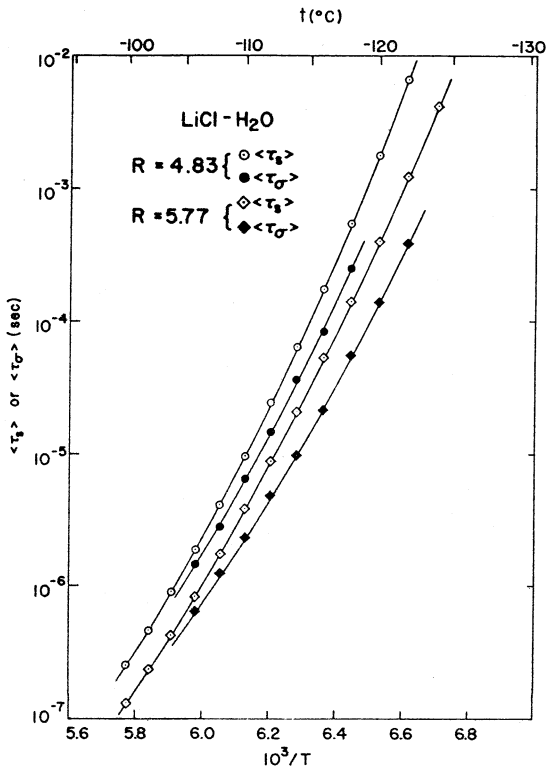

Figure 9. Conductivity and shear relaxation times for two noncrystallizing aqueous LiCl solutions, showing similar super-Arrhenius behavior for the different relaxation times. The enthalpy relaxation times, determined from analysis of the glass transition endotherm (seen in Figure 1 for calcium nitrate solutions) yield somewhat longer relaxation times than, but similar temperature dependences to, the shear relaxation times (reproduced from ref 28 with permission. Copyright 1971 American Physics Society).

When followed over wide enough ranges of temperature, such behavior is usually found to change over, at high temperatures, to a much less temperature-dependent form and eventually to settle down to a simple Arrhenius demeanor with a physically sensible pre-exponent of about 10^{-14} s, in the case of relaxation times.[145,146] The strong curving of the overall Arrhenius plot is typical of the "fragile" liquid. Nonfragile (or "strong") liquids show simple Arrhenius behavior, with physical pre-exponents, over the whole viscosity range from the glass temperature to the high fluidity state. There are currently no examples of nonfragile molecular liquids, now that water's apparent nonfragile behavior near 136 K seems to be because it is not a liquid at all but, rather, a glass (as seen in the previous section of this paper). However, nonfragile behavior is seen in certain multicomponent aqueous systems as will be seen below.

The study of fragility in aqueous systems is of particular interest because of the special volumetric behavior of aqueous systems of high water content. Fragile glass-former behavior can be seen in aqueous systems that have domains of negative expansivity.[147] This immediately rules out any simple free-volume type interpretation[148] of the super-Arrhenius behavior in aqueous systems, and forces attention on alternative approaches.

An example of moderately fragile behavior in an aqueous solution is shown in Figure 9 based on the studies of shear viscosity and conductivity relaxation in LiCl solutions by Moynihan et al.[28] These workers converted the raw viscosity and conductivity data to relaxation times so that the two properties could be compared in the same units. This was done using (i) the Maxwell relation between viscosity and relaxation time

$$\eta = G_\infty \tau_s \tag{1}$$

where G_∞ is the infinite frequency shear modulus, and τ_s is the shear relaxation time, and (ii) the equivalent of the Maxwell relation for ionic conductivity

$$\sigma = e_0/M_\infty \tau_\sigma \tag{2}$$

where e_0 is the permittivity of free space, and M_∞ is the infinite frequency electrical modulus.[149]

The Arrhenius plot shows that the two times are rather similar until the temperature approaches T_g when the conductivity shows a tendency to relax more quickly. A third data set is available[150] for the enthalpy relaxation time obtained from phenomenological model analysis (Tool-Narayansamy-Moynihan[16]) of scanning calorimetry data (like those of Figures 1 and 2) through the glass transition for the compositions of Figure 9. The enthalpy relaxation time is found to be the most slowly relaxing property of the three. When such measurements are carried out on single component liquids, e.g., glycerol, all three properties are found to have the same relaxation time.[151,18] This suggests that aqueous solutions of electrolytes, not surprisingly, have a more complex structure and dynamics than that of simple liquids.

The temperature dependences of the shear and enthalpy relaxation processes are closely similar, so the fragility of the solution, assessed by the methods discussed below, would be equally similar. The conductivity, on the other hand, shows a weaker temperature dependence near T_g than do the others. In some cases of solvent-free ionic liquids, the difference in relaxation times can become very large—many orders of magnitude, in fact. Moynihan et al.[28] defined the decoupling ratio $R = \tau_s/\tau_\sigma$ to quantify this decoupling of the conducting modes from the structural relaxation modes, and the concept has since been widely used in the science of glassy solid electrolytes.[152] A significantly greater decoupling of conductivity from viscosity was found in the case of $Ca(NO_3)_2-H_2O$ solutions.[22] These solutions also exhibit rather greater departures from Arrhenius behavior than seen in Figure 9, and hence are to be regarded as more fragile. In fact, with the exception of D,L-lactic acid, the solution of calcium nitrate with 4 mol of water (i.e., molten $Ca(NO_3)_2 \cdot 4H_2O$) is the most fragile congruently melting compound known, and the solution with 8 molecules of water per Ca^{2+} ion proves even more fragile.[22]

To display the relative fragilities of different liquids, it is helpful to present the data in a scaled form. This may be done using the temperature at which the liquid has a chosen value of the property under study (e.g., viscosity) as a scaling parameter for the temperature axis of the Arrhenius plot.[3] Such plots, which are close relatives of Figure 10 below, have

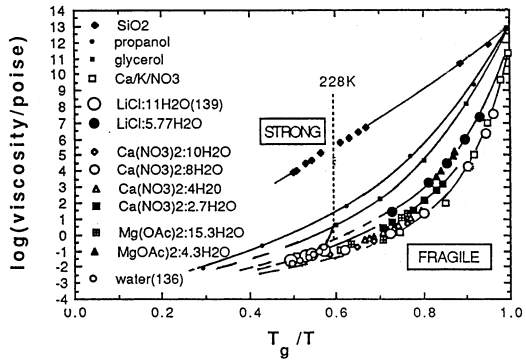

Figure 10. The T_g scaled Arrhenius presentation of viscosity data for a variety of aqueous solutions showing the effect of the second component on the fragility of the solution. The scaling temperature is the calorimetric glass transition temperature (onset T_g at 10 K/min scanning). The vertical dotted line represents the power law divergence found for supercooled pure water, plotted using the T_g value 136 K. (Adapted from ref 120 by permission. Copyright 1994 Blackwell Science.)

become quite well-known in recent years. Although there are critics of the practice of using an internal liquid property, namely, a particular viscosity or relaxation time, as the basis for scaling, there really is no satisfactory alternative. The use of a thermodynamic transition point such as the melting point has of course been proposed, but quickly abandoned because of the tremendous range of viscosities that different substances exhibit at their melting points. No helpful ordering of complex behavior patterns is gained thereby. Indeed, it is only the liquids that have high viscosities at their melting points that can successfully be supercooled to the glassy state.[144] (This self-selection, leads to the "2/3 rule" ($T_g \approx 2/3T_m$) which is actually a tautology, because exceptions either do not vitrify or do not crystallize, hence do not get counted). An internal thermodynamic transition temperature, the Kauzmann (ideal glass) transition temperature where excess of liquid entropy over crystal extrapolates zero[153] could make an appropriate choice of scaling parameter. However, this temperature can only be obtained by extrapolation. In any case, the thermodynamic data needed are mostly unavailable, and the existence of an "ideal" glass transition, though attractive, is very controversial.[154−156] Kauzmann himself[153] did not believe it exists.

While the original fragility plots[3] used the temperature at which the viscosity reaches 10^{12} Pa·s as the scaling temperature, this proves not to be the most useful choice. There are many cases in which the measurement of a viscosity near T_g is difficult, whereas the measurement of the T_g itself is simple and also fairly unambiguous once the alternative possible definitions have been properly considered (Figure 2 and caption). Because the T_g used in this work (Figure 2) is always found to correspond to a fixed value of the structural relaxation time, ~100 s,[16] an attractive alternative to scaling by the temperature of constant large viscosity is therefore to use the measured (onset) T_g as the scaling parameter. An example of this type of fragility plot is shown in Figure 10 for a variety of aqueous solutions of the electrolyte type and includes the two cases already discussed. A corresponding plot for nonelectrolyte solutions will be seen later.

The form of these plots is usually rationalized in terms of the well-known three parameter Vogel−Fulcher−Tammann (VFT) equation, written in the form

$$\eta = \eta_o \exp(DT_o/[T - T_o]) \quad (3)$$

where η_o, D, and T_o are constants. Increases in the value of D between about 5 and 100 change the curvature of the plots between fragile and strong extremes.

In the concentrated electrolyte solutions, particularly those of multivalent cations, the value of the scaling parameter T_g changes very strongly with composition (as seen in Figure 4). With molecular second components, the changes are generally milder because the second components themselves have low T_g's. Solutions of the di- and trisaccharides, and water-soluble polymers, on the other hand, have strongly composition-dependent scaling parameters (see Figure 3).

To quantify the fragility, various approaches have been taken. A quantification is desirable because it has been found[100,157,158] that, once the fragility of a glassformer is known, many other characteristics can be predicted. An obvious manner of quantifying the fragility would be to use the parameter D of eq 3 (or rather its inverse, $F_{VFT} = 1/D_{VFT}$) since the D parameter describes the curvature. However, eq 3 rarely fits the data over the full range from fluid to glass within their random errors, so the value of the fragility obtained in this manner will depend on the range of data fitted. The problem is most severe for the most fragile liquids. The same problem applies to the use of the ratio T_g/T_o, which is related linearly to the parameter D[3b].

A common way of dealing with this problem is to avoid any equation-fitting and simply to measure the slope of the Arrhenius plot near T_g. This is called the "m" fragility or "steepness index,"[159] i.e.,

$$m = \mathrm{d}\log(\tau)/\mathrm{d}\log(T_g/T)_{Tg} \quad (4)$$

The m fragility is therefore related to the conventional Arrhenius activation energy for the process under study, E_a, by the expression

$$m = E_a/2.303RT_g \quad (5)$$

m can be expressed in terms of the parameters of the VFT equation, when the latter is constrained to have a pre-exponent of 10^{-4} poise (10^{-5} Pa·s) by

$$m = m_{min} + m^2_{min} \ln 10/D = 17 + 590/D \quad (6)$$

The constraint fixes m_{min} at 17 for viscosity and 16 for relaxation time, the difference between the two coming from the temperature dependence of the proportionality constant G_∞ (eq 1). A disadvantage of this quantification is the frequent lack of data near T_g and the difficulty of measuring this slope accurately, though the use of the fictive temperature method for enthalpy relaxation measurements,[99]

particularly in a current form,[160] goes some way toward removing this objection.

Recently,[158,161] there has been a proposal to avoid both equation-fitting and slope measuring problems by defining fragility directly from data obtained at intermediate viscosities (or values of dielectric relaxation time etc) using the $F_{1/2}$ fragility. We illustrate it for the case of relaxation time data. The $F_{1/2}$ fragility is obtained by first finding the temperature at which the relaxation time is halfway (on log scale) between the high-temperature value and the value 10^2 s characteristic of the glass transition, under the assumption of a fixed high-temperature limit to the relaxation time of 10^{-14} s, as indicated empirically by plots such as Figure 9. $F_{1/2}$ is then defined so as to lie between 0 and 1.0 by the relation

$$F_{1/2} = 2T_{1/2}/T_g - 1 \quad (7)$$

where $T_{1/2}$ is the temperature at which $\tau = 10^{-6}$ s (e.g. 165.5K for LiCl·5.77H_2O). Note that this definition is based directly on the deviation from the Arrhenius law, which is the phenomenon that motivated the fragility concept in the first place.

No definition of fragility is free from ambiguities. For instance, viscosity for molecular liquids does not have the value 10^{13} poise at T_g. Therefore, it is ambiguous which value of viscosity to use in obtaining $T_{1/2}$. Maintaining a consistent reference temperature would seem to be the primary consideration. Thus, in seeking correlations between kinetic fragility and thermodynamic fragility, recently,[162] we used the temperature at which the viscosity reached the value $10^{3.5}$ Pa×e1·s midway between 10^{12} and 10^{-5} Pa·s, even though the high value was not yet reached at T_g for many cases.

For dielectric relaxation times, the $\tau_{1/2}$ value is clearly 10^{-6} s. This case[159] is not ambiguous because the enthalpy relaxation time at T_g (onset) is the same as that used to define the scaling parameter T_g (for a standard scan at 10 K/min).

The relation between $F_{1/2}$ and the m fragility is a simple one,

$$F_{1/2} = (m - 16)/(m + 16) \quad (8)$$

where again, 16 orders of magnitude is assumed to separate T_g from the high-temperature extreme for relaxation and 17 would be used for the case of viscosity. When m determined at $T_{1/2}$ using this relationship is not the same as m determined at T_g, then it means that eq 3 cannot apply with a physical value of the pre-exponent, even in the lower half of the range between T_g and $T_{1/2}$. This is the range in which the relaxation behavior is thought to be dominated by the energy landscape,[18,163−165] so some unusual features in the landscape energy distribution would be implied.

(b) Electrolyte Solutions

(i) Complex Systems with Fragile/Strong Crossovers

We can find evidence for complexity in the energy landscape for aqueous solutions, using solutions from the same system that we used, in Figure 9, to introduce the fragility behavior. The viscosity data, that were converted by Moynihan et al. to the relaxation times plotted in Figure 9, are shown in Figure 10 as solid circles for the case of the $R = 5.77$ solution. From Figure 9, a value for $T_{1/2}$ at log $\tau = 10^{-6}$ s was found to be 167 K, and the value of T_g for the solution is 138 K (which compares well with the temperature at which the relaxation time in Figure 9 extrapolates to 100 s (137.4 K)). From these values, we obtain a $F_{1/2}$ fragility of 0.65. Using eq 8, we then expect a value of m of $16(1 + F_{1/2})/(1 - F_{1/2})$, or $m = 75$. However, a value of 60 is found from DSC studies[166] using the method of Moynihan et al.[27] This discrepancy might seem alarming, but much worse is encountered at higher water contents.

For instance, it is seen in Figure 10 that, from viscosity data, the solution of stoichiometry LiCl·11H_2O ($R = 11$) should be much more fragile than the $R = 5.77$ solution we have just considered. If the latter has an $F_{1/2}$ fragility of 0.65, then the value for the $R = 11$ solution should be 0.7 and the corresponding m value should be 85—quite fragile. However, the values for m measured at T_g by the DSC method trend in the opposite direction, fragility decreasing with increasing water content (increasing R value). At $R = 9$, m is found to be ∼45 [166], and extrapolation would indicate values below 40 at $R = 11$. Actual behavior at $R = 11$ is difficult to evaluate because the glass transition changes shape, possibly associated with the separation of a second liquid phase as discussed in section IIc.

The trend with increasing water content, to higher fragility at high temperature but lower fragility at low temperature, implies that there is a crossover in the behavior of the viscosity during cooling. This is consistent with the finding[120,167] that eq 3, fitted to the high-temperature viscosity data for the more dilute solutions in the glassforming range, yields values of T_o in excess of T_g, which is unphysical. These findings can be summarized by the assertion that, in the dilute solutions of LiCl in water, there is a "fragile-to-strong" transition, just like recent work[168] reports for liquid silica. Liquid silica has a weak density maximum at about the same T/T_g value as does $R = 10$LiCl solution.

In the case of SiO_2, we know the reason for the crossover, thanks to the simulations of Poole and coworkers.[168] In the case of SiO_2 at zero pressure, unlike previous cases of mixed Lennard-Jones systems, the distribution of inherent structures is not Gaussian in energy, but something more complicated, which causes a maximum in the heat capacity to occur, below which strong liquid behavior ensues. It seems possible that when a Gaussian energy distribution controls the thermodynamics, a VFT equation describes the kinetics over the whole range, up to the temperature where the system has been "floated," by temperature increase, to the top of its landacape. Beyond this temperature, the behavior becomes Arrhenius.

Since a density maximum is strongly associated with the build-up of hydrogen bonded clusters in the case of pure water, it is tempting to see the behavior of the solutions as a precursor to the strong-to-fragile

transition proposed to occur in water.[12,169,170] While this transition was initially proposed on the supposition that behavior observed in ASW above 136 K was *liquid* behavior, it is now[170] shown to apply to water in the range 150−236, based on thermodynamic observations (see section IIIb). The thermodynamic argument requires that the fragile-to-strong transition on cooling in pure water has a sharper form than manifested in SiO_2 or in the aqueous solutions. Unfortunately, it is not directly observable because of fast crystallization kinetics near the crossover temperature.

It is worth mentioning that this fragile-to-strong transition occurs not only in LiCl solutions but also in lithium acetate solutions near the edge of the glassforming region. In the acetate case, it is known that the glass transition occurs in a temperature domain where the expansion coefficient is still negative, because T_g *decreases* with increasing pressure.[171] An Ehrenfest-like relation known to be valid for most glassforming liquids and solutions[172] relates the pressure dependence of T_g to the expansion coefficient by

$$dT_g/dP = VT\Delta\alpha/\Delta C_p \qquad (9)$$

where $\Delta\alpha$ is the change in expansion coefficient at T_g and must be negative, since ΔC_p cannot have a negative value.

(ii) Simply Behaving Systems

Contrasting with the complexity of the Li salt solutions are the solutions of $Ca(NO_3)_2$. In this case, the values of T_o of eq 3 fall a physically sensible distance below the T_g values at all glass-forming compositions. Furthermore, where there is a congruently melting compound (at $R = 4$) for which the appropriate thermodynamic measurements have been performed,[25,172] the value of the Kauzmann temperature T_K coincides with the value of T_o.[116b] Results for this simple system are shown in Figure 11.

Figure 11 shows the variation with temperature of the three temperatures which together characterize the glassforming properties of the system. The first is the temperature that, more than any other, determines whether explorations of the glassforming properties can be made in the first place. This is the homogeneous nucleation temperature T_h marked on the water-rich side of the diagram. Below this temperature, crystallization is rapid and inevitable unless the solution is hyperquenched. The glassforming range is determined by T_h plunging below the second of the characterizing temperatures, namely, T_g, as seen in Figure 11 at about 6.6 mol % salt (14 waters per cation). It is notable that if the formation and growth of homogeneous nuclei did not become so slow near T_g, the temperature at which they become probable would plunge below T_o, the third characteristic temperature, and then crystallization would not occur even on infinite time scales. T_o is the temperature at which the relaxation time would diverge, according to eq 3. In the case of $Ca(NO_3)_2$−H_2O solutions this temperature remains a fixed fraction of the experimental T_g over the whole range,

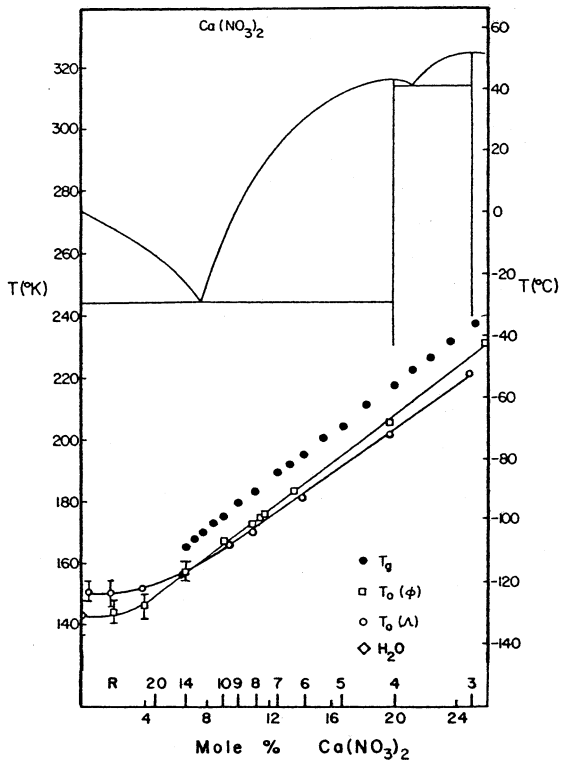

Figure 11. Variation of the glass transition temperature, and the ideal glass temperatures obtained from VFT equation fitting of conductivity (Λ) data and fluidity (∅) data, for aqueous solutions of calcium nitrate. The coincidence of T_o with the Kauzmann temperature, T_K, obtained from thermodynamic data on the congruently melting compound $Ca(NO_3)_2{\cdot}4H_2O$, is shown by the cross-in-circle symbol at this stoichiometry. The ratio of T_g/T_o(∅) remains almost constant, implying that the fragility is constant with composition, as seen in Figure 10. The curve marked T_H shows the behavior of the homogeneous nucleation temperature for ice, below which crystallization cannot be suppressed except by rapid quenching. When T_H falls below T_o, crystallization becomes kinetically constrained in clean solutions.

indicating a constant fragility according to the relation[3b]

$$T_g/T_o = 1 + 0.0255D \qquad (10)$$

which applies when $\eta_o = 10^{-5}$ Pa·s and $\eta_{Tg} = 10^{12}$ Pa·s.

Since (a) T_o accords well with the Kauzmann temperature, as already noted (see the large cross-in-circle symbol in Figure 11) and (b) the preexponent for the structural relaxation time indicated by the data of ref 22a is close to the physical value 10^{-14} s (inverse quasilattice vibration time), it seems that these solutions behave in an almost ideal fragile fashion. They should therefore serve as appropriate systems on which to test models for the configurational excitation of glasses into fragile liquids, and some discussion of this matter will be given in a later section. First, it is appropriate to consider the phenomenology of aqueous *non*-electrolyte solutions.

(c) Nonelectrolyte Solutions

There have of course been many studies of nonelectrolyte solutions containing water, but the num-

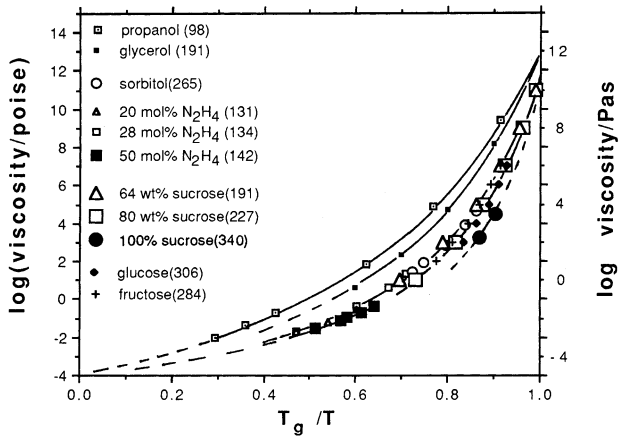

Figure 12. T_g scaled Arrhenius plot of the viscosities of nonelectrolyte solutions showing how, despite the extensively hydrogen bonded nature of such solutions, none are less fragile than glycerol. In both hydrazine-containing, and sucrose-containing, solutions, the fragility decreases with increasing water content. The values for pure sucrose are uncertain because of the probability of partial decomposition of the samples.

ber from which solution fragilities can be obtained is few. Many of the latter have been aqueous sugars because of the interest in food and tissue preservation technology, and the importance of sugar solutions in food processing. Viscosities for selected molecular solutions are shown in Figure 12[120] along with data for the intermediate liquids glycerol and propanol. The latter provide a visual basis for the observation that, as with electrolytes, the molecular solutions tend to be fragile in character. In the case of the sucrose solutions, the data cover a wide viscosity range and the fragility is seen to decrease slowly as the water content increases. The fragility of pure sucrose is probably high as indicated, $F_{1/2} \approx 0.82$, but the difficulty of avoiding decomposition of the anhydrous melt is enough to render any conclusions uncertain. Within limits set by the same source of uncertainty, the entropy-based thermodynamic fragility is also very high.[17]

Additional information on the fragility of disaccharide aqueous solutions is available from the NMR studies of Ludemann and co-workers[174−176] who used NMR methods to follow separately the relaxation of water and sugar molecules in variable concentration solutions of a variety of mono- and disaccharides. They found that each could be described by eq 3, but that at higher concentrations, the T_o value for the water was much lower than that for the sugar molecules, again indicating the complexity of aqueous solutions. The implications of these studies is that water molecules can decouple from the solution containing them, like the fast ions in the $Ca(NO_3)_2$ solutions could decouple from the structural relaxation. The decoupling seems to occur with respect to both rotational and translational motions, and the degree of decoupling varies strongly with the solution composition and differs from sugar to sugar apparently maximizing for trehalose. Related results, indicating separate decoupled transport channels for both water molecules and small ions, are reported by de Pablo and co-workers.[67,176]

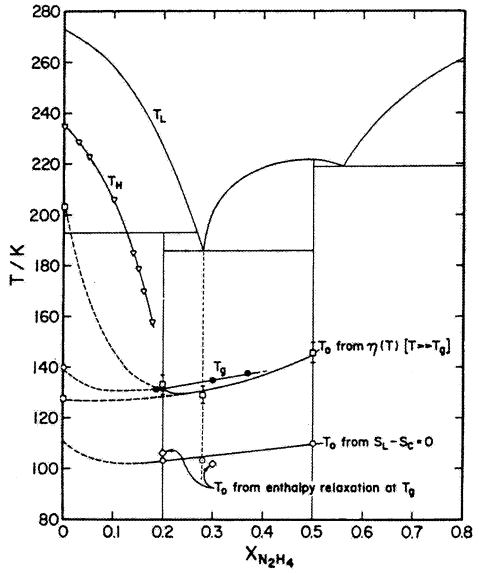

Figure 13. Phase diagram for the system $H_2O + N_2H_4$, showing also glass transition temperatures, T_g, eq 3 (VFT equation) T_o parameters from low viscosity data of and Kauzmann tempertures obtained for the two compounds and the eutectic (see text for assumptions involved).

Ludemann and co-workers measured viscosities of the same solutions and found that the eq 3 T_o parameters for the sugar diffusivity and the solution viscosity are the same, and the D values indicate high fragility,[174] in accord with the indications of Figure 11. T_o values for the water, on the other hand, were found to be much lower and less concentration-dependent, indicating independent relaxation paths.

There is a whole field of freeze-dried aqueous glassy systems involving water-soluble biomolecules, with or without sugar protective components, for which the fragility seems to be important to the active lifetime,[177] because of the correlation of aging behavior with fragility. The role of decoupled motion of water molecules in stabilization of biomolecules is one that needs detailed attention.

In the case of the hydrazine solutions shown in Figure 12, additional information is available. This binary system exhibits two compounds, one of which is congruently melting hence available for Kauzmann analysis. However, even for incongruently melting compounds, it is possible to extract a Kauzmann temperature that is thermodynamically valid within the uncertainties of extrapolation below T_g.[178] Furthermore, there exists a eutectic temperature at which a solid(s) to liquid transformation occurs isothermally. If the entropy of mixing contains no temperature-dependent component then this fusion entropy can also be used, together with the appropriate heat capacity data to extract Kauzmann temperatures. Thus, three Kauzmann temperatures can be extracted from thermal data on this system.[179] These are displayed in Figure 13, where they are compared with the values of T_o extracted from (i) the high temperature viscosity data of ref 120 and 167, and (ii) the relaxation of the enthalpy near T_g measured by the Moynihan method referred to in the earlier discussion of $LiCl-H_2O$ solutions. Again the same finding is made. T_o is lower when measured near T_g,

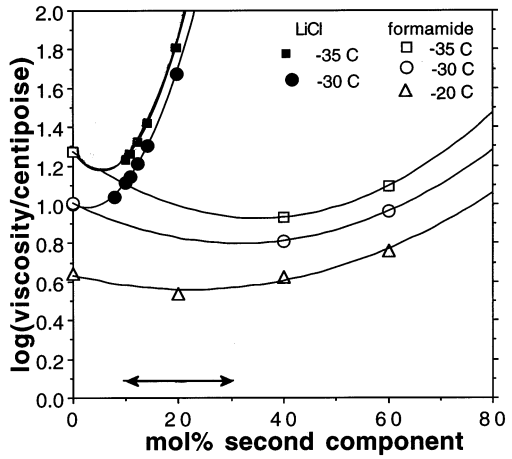

Figure 14. Viscosity isotherms for stable and supercooled aqueous electrolyte and nonelectrolyte solutions, showing minimum values and implying rapidly increasing viscosities and also glass temperatures in water-rich solutions, as argued earlier with the help of Figure 7. Solid curves through lines are all third order polynomial best fits.

so the fragility assessed at high temperatures appears greater than when assessed near T_g. The values of T_o measured near T_g are validated by their close proximity to the Kauzmann temperatures. For these cases, $T_g/T_o \approx 1.26$, a little less than for glycerol. For data taken in the range $T = -35$ to $+50$ °C, on the other hand, $T_g/T_o \approx 1$. Such values imply $m \approx 8$, so again there is a strong change in curvature with decreasing temperature. The m value near T_g is not small enough to warrant a description of fragile-to-strong "transition", as for the $LiCl-H_2O$ solutions. However, the trend is in the same direction.

It is therefore of interest to examine the behavior of the viscosity itself, as a function of composition into the composition range where crystallization prevents measurements near T_g. Data are shown at −20 and −35 °C for both hydrazine and LiCl solutions in Figure 14. The glassforming composition range for LiCl solutions is indicated by a double headed arrow. For hydrazine solutions the glassforming range is 19−39 mol % N_2H_4. Both systems show minima, the viscosity rising sharply in the case of LiCl solutions. Since the glass transition is often thought of as an isoviscous phenomenon, both data sets indicate that the glass temperature should start to rise again in the range between pure water and the edge of the glassforming range, as suggested by Figure 7, seen earlier.

(d) Models for the Fragility

The reason some liquids are fragile and others not, while still others change from fragile to strong during cooling, is not at all clear despite much interest in the matter. Here we briefly review some possibilities. Any model for non-Arrhenius transport behavior near T_g is potentially a model for fragility.

For instance, viscous slowdown is popularly explained by mode coupling theory, MCT,[180] in which viscosity diverges at a critical temperature T_c(MCT) according to a power law in temperature. In this approach, the fragility is determined by the factor that fixes the exponent of the power law, which itself traces to the temperature dependence of the structure factor. However, the power law only describes behavior at temperatures far above T_g because the predicted divergence does not happen. At the predicted T_c the actual relaxation times are of order 10^{-7} s, rather than infinite. The temperature T_c is now known as the "crossover" temperature because the dynamics of fragile liquids indeed usually undergoes some change in character at this temperature. Values of this temperature for aqueous solutions were first given by Taborek et al.[180c] An ideal glass transition in the MCT sense only occurs in systems with infinite energy barriers. Thus, the mode coupling expressions are not useful for interpreting fragility. Models for the VFT equation, eq 3, are more relevant, and there are several of them.

The simplest of such models is perhaps the free volume model of Cohen and Turnbull mentioned earlier.[118] In its earliest and most popular form, this was a model to explain the empirical Doolittle equation[181] for the viscosity of molecular liquids

$$\eta = \eta_o \exp(v^*/v_f) \qquad (11)$$

where η_o is the preexponential constant and v^* is a constant found to be of the order of the molecular volume. v_f is a volume, the free volume, which is small with respect to v^* but which increases as the temperature increases above T_g. It tends to zero at a temperature T_o somewhat below T_g. The model gave an account of how an exponential relation between temperature and free volume could arise but did not provide an explanation for the rate of increase of the free volume itself. Therefore, the free volume model is not a useful model for fragility because the fragility, in this model for the eq 3, is determined by the temperature dependence of the free volume. In any case, the behavior near the glassforming boundary, where the expansivity is negative, is difficult to rationalize in terms of free volume concepts.

While it is free of the latter problem, the problem concerning dv_f/dT afflicts another popular model for the non-Arrhenius character of liquid relaxation, the Adam Gibbs "entropy"equation.[182]

$$\eta = \eta_o \exp(C/TS_c) \qquad (12)$$

Here the thermodynamic quantity controlling the temperature dependence of the relaxation time is the configurational component of the total entropy, and the understanding of the fragility therefore requires an understanding of the magnitude of the configurational heat capacity. While this was parametrized in the earlier Gibbs-Dimarzio theory[183] in terms of hole energies, chain stiffness, and lattice statistics, the theory was formulated for polymers and its adaptation to simple liquids was not undertaken. The configurational heat capacity may be considerably less than the total excess heat capacity (i.e., the difference between crystal and liquid values), and this difference is usually not taken into account in testing the theory for correct functional form. The Adam Gibbs theory cannot become a theory for liquid

fragility until a model for the heat capacity is formulated.

Attempts to model the heat capacity of liquids in terms of more fundamental quantities have been surprisingly rare. Most have involved some type of two-state model, in which the verbal description varies but the algebraic expressions remain the same.[184−187] The species are assumed to mix ideally (i.e., excite noncooperatively), implying a binomial distribution of energy states. Relaxing this requirement,[187] i.e., allowing for cooperativity in the excitation process, makes it possible to account for first-order phase transitions between liquid states of different character, as is suggested to happen in water above a critical pressure.[123−126,133−135] This was discussed earlier (section 11bii) in connection with polyamorphism in vitreous water. A related case is that discussed by Granato[187d] except, in that case, the phase transition envisaged is between crystal and liquid states.

For the specific case of water a variety of lattice models yielding the heat capacity have been developed.[188−192] These are microscopic theories whose lattice bases permits a precise Hamiltonian to be written down in each case. Consequently many results can be obtained. The thermodynamic behavior of these models have been fully worked out (yielding singularities and critical points[188−189] or the specific absence thereof[190,191]) so incorporation of entropies in eq 12 could be carried out in much the same way as is done with experimentally derived functions in the final section of this review. However, because they are specific to water they will not be discussed further here.

An alternative and more sophisticated version of the noncooperative n-state type of model is the "correlated site" model of Stanley and Teixeira,[195] developed for the specific case of water. In this model, there are five distinct species depending on the number of bonds connecting a given molecule to others, and interest is focused on the percolation of the four-bonded (tetrahedrally coordinated) molecules. Tested by computer simulations, using an energy cutoff to define the species, the distribution of species was indeed found to conform to a binomial distribution.[196,197] The model predicted thermodynamic properties, and hydrogen bonded species lifetimes, the longest of which was for the four-bonded molecules. Four-bonded molecules tended to accumulate in patches that grew in size with decreasing temperature. Gel-like bond percolation occurred at quite high temperatures where the water is still highly mobile, due to the short lifetime of the bonds. Percolation of four-bonded patches would imply long-lived structures hence glass formation. The bond lifetime followed an Arrhenius law. The rearrangement mechanism was shown to involve a transiently five-coordinated state, which could be trapped at low temperatures,[198] though this species was not included in the original model.

The only one of the above that has been applied to the case of super-Arrhenius, glassforming aqueous solutions has been the excitations model of Angell and Rao,[185c] in which it is supposed that the potential energy of an amorphous system can be increased by the excitation of elementary packing modes. These are treated as "bonds" that can be either "on" or "off" and it was assumed, for calcium nitrate solutions,[24b] that the excited states are independent, so simple two-state statistics applies.

Once the number of elements in the bond lattice per mole of substance has been decided, the thermodynamic fragility is found to be determined exclusively by the entropy change directly associated with the excitation.[155] This elementary excitation entropy, ΔS per mole, is to be distinguished from the entropy increase arising from distribution of excitations across the possible sites in the bond lattice.

To apply this sort of model to the viscosity of aqueous solutions, Angell and Bressel[24b] substituted a configurational excitation for the volumetric excitation of eq 11, to obtain

$$\eta = \eta_o \exp(x^*/X_B) \tag{13}$$

where X_B is the degree of excitation, at temperature T, above the configurational ground state, and is a simple function of the free energy of excitation

$$X_B = 1/(1 + \exp(\Delta G/RT)) \tag{14}$$

where ΔG has enthalpic, ΔH, and entropic, $T\Delta S$, components.

The viscosity is thus described, alternatively to eq 3, by a transcendental equation

$$\eta = \eta_o \exp (c^*/[1 + \exp \Delta G/RT]) \tag{15}$$

which contains both thermodynamics and dynamics. The critical excitation parameter x^* may be set to unity (equivalent to setting v^* in eq 11 to the molecular volume), to yield an equation with three parameters (η_o, ΔH, ΔS). This simplified version accounts[24b] for the non-Arrhenius behavior seen in Figure 10 as well as can be achieved with the three parameter VFT equation, eq 3. Equation 15 has the advantage that two of the three parameters also account for the increase in heat capacity through the glass transition after a number corresponding to the number of excitable (rearrangeable) structural units per mole of substance is introduced. The number required to fit the data for liquid $Ca(NO_3)_2{\cdot}4H_2O$ is 9, which is reasonable. It is intermediate between the number of moles of individual molecular and ionic entities per mole of solution, 7, and the number of "beads" in the sense of Wunderlich's definition[199] per formula unit, which is 11. The excitation parameters are also reasonable, $\Delta H = 10.7$ kJ/mol, $\Delta S = 21.9$ J/mol·K (a typical small molecule entropy of fusion).

The strength of this simple model is that, in seeking to interpret fragility, it focuses attention on a single quantity, the excitation entropy. It therefore inspires the question of whether the origin of fragility lies in the vibrational manifold,[185] or in the configurational manifold of states. This is something that in principle can be decided by experiment, and neutron scattering studies to provide answers are currently in progress. The weakness of the model is that by restricting the system to explore just one type

of excitation and by disallowing interactions between excitations, a maximum in the excess heat capacity is forced on the system, and this is not seen in the majority of simple liquids and solutions. The excitations model therefore fails in the same way as does the Einstein heat capacity model of solids, insofar as it fails to deal with the collective nature of the excitations.

The heat capacity maximum is associated with an inflection in the excitation profile described by eq 14. A related consequence, sometimes seen as an advantage, is that the state of excitation, hence also the excess entropy, goes continuously to zero and the Kauzmann crisis is thereby resolved. However, if the binomial distribution assumed in the excitations model is replaced by the Gaussian distribution assumed in the random energy model[200] and supported by simulation studies,[201−203] then the heat capacity maximum would be eliminated and the Kauzmann singularity would be restored.

In the case of water itself, no simple excitation scheme can hope to describe the extreme fragility of the supercooled state,[12] though cooperative excitation models,[187] and lattice models[188−191] have the potential to do so. Simulation studies,[203] show that there is an important role for the vibrational modes (basin shape effect) in determining the rate of excitation, hence also the fragility, even at constant volume. The extension of such studies to solutions should help clarify the sources of high fragility in cases such as $Ca(NO_3)_2-H_2O$.

(e) Fragility of Pure Water

A problem of quantifying the fragility of water itself is that the value of the scaling parameter in the temperature axis, T_g, of the fragility plot (Figure 10) keeps changing with time, as discussed in the second part of section II. Most representations of water on a Figure 10 type diagram have been based on the previously accepted value $T_g = 136$ K. However, we have demonstrated in the first section of this review that this value is probably incorrect. If water requires a higher characteristic T_g to reconcile its behavior with that of other liquids (through the behavior of their glasses formed on the same time scale), then its position on the Figure 10 plot must be changed. It must be shifted along the horizontal axis to higher T_g/T. Irrespective of the temperature appropriate for T_g, however, it is clear from the date available for viscosity to −35 °C, that its behavior must be rather different from that of other liquids.

The form of the viscosity Arrhenius plot for water at temperatures below the homogeneous nucleation temperature, −40 °C, can be deduced within broad uncertainty limits, by application of a modified Adam-Gibbs equation.[182] The Adam-Gibbs equation enjoys a good reputation for correlating viscosity and relaxation data with thermodynamic data for molecular liquids.[204−208] Before using this correlation to discuss the fragility of water relative to those of other liquids, it is necessary to consider two problems that are currently under discussion.

The first of the two problems concerns the entropy to be used in the Adam-Gibbs equation. The configurational entropy invoked in the Adam-Gibbs theory is most simply to be thought of as the ideal mixing entropy term in a two-state system. More accurately, it is represented by $k_B \ln W$ where W is the number of distinct "basins of attraction" on the potential energy hypersurface ("landscape") for the particulate system.[163,164,209,210] This entropy has been evaluated recently[163b,212] by researchers using computer simulation methods to determine quantitative aspects of the "inherent structures" that characterize different systems. This quantity is demonstrated, in these simulations, to be different from the "excess entropy". The excess entropy is the difference in entropy between the liquid and any single one of the low energy glassy structures in the simulated simulations. The crystal can be thought of as the entropic equivalent of any single one of the lower energy glasses. (The essential feature is that the structure remains unchanged over wide temperature ranges). It is the state generally used to assess the excess entropy of the liquid over glass (e.g., for Kauzmann temperature evaluations).

Particularly when the system considered is a constant pressure system, the configurational entropy is rather different from the excess entropy. This is because the basins of attraction populated at the higher temperatures have very different vibrational densities of states than those populated at low temperatures. Therefore, the excess entropy may be much in excess of the configurational quantity, and is not the quantity called for by the Adam-Gibbs theory. However, it is the quantity that has been used to test the theory in practice.[213−217] Since these tests have usually been successful, at least for a considerable range above T_g, it must be concluded that there is an empirical equation connecting the excess entropy to the diffusivity. As we have detailed elsewhere,[218] the reason that this form of the Adam-Gibbs equation gives a good account of the data is that the two entropies, S_c and S_{ex} are constrained by their nature to change proportionally over temperature. Regardless of the truth of the latter statement, it is reasonable to test relationships using the "modified" Adam-Gibbs equation in which, faute-de-mieux, the excess entropy is employed.

The second problem is to obtain the excess entropy behavior for water in the range of temperatures below the temperature where the equilibriated, or supercooled, liquid heat capacities have been measured. This latter problem has been the object of a recent analysis by Starr et al.[112] These workers used measurements of the free energy of amorphous water at 150 K (obtained by Speedy, Kay and co-workers[219] from vapor pressure measurements), together with measurements of the crystallization enthalpies of amorphous and annealed hyperquenched glassy water,[93] to obtain a measure of the entropy of water at 150 K. Between this temperature, and that where the entropy is known from measurements made in ergodic conditions, the entropy can vary in only a limited range of ways without violating thermodynamic constraints. The mean of this band of thermodynamically allowed variations is shown in Figure 14a, in comparison with the variation of the measured excess entropy, scaled by the value at the

calorimetric glass transition, for a variety of other liquids as recently reported.[17] There are two curves for the water data, one for the generally accepted T_g value 136 K[85,92] and one for the new assignment 165 K.[14]

The temperature variation of the diffusivity of water according to the Adam-Gibbs equation, when modified by the use of S_{ex}, and parametrized by fitting to experimental data in the regime above 235 K, is shown in Figure 14b. The sigmoidal shape of the excess entropy curve imposes a sigmoidal form on the log diffusivity vs $1/T$ plot. Such a variation would render water distinct from all the other liquids in this comparison and would substantiate the notion that water undergoes a transition from extreme fragility in the range 240−273, to strong-liquid character in the range where crystallization is very probable. It is notable that, in the cases of silicon and germanium, it is the transition from high-temperature fragile to low-temperature strong character via a first-order phase transition that is responsible for the rapid crystallization.[138b,220,221]

So long as it seemed that there was an observable region of supercooled liquid existence between 136 K and the crystallization at 155−160 K, it made sense to talk about this interpolated viscosity behavior. However, in view of the unfortunate conclusion, from section 3, that this range does not exist in reality for bulk water samples, it becomes rather unphysical to discuss such normal time scale viscosity behavior derived in this manner. The only viscosity vs temperature relation that it is physically meaningful is one that could, in principle, be observed by some exotic technique, applied during cooling at the extremely high rates that allow crystallization to be bypassed. In a sense, that is what is being measured in the enthalpy relaxation experiment of Figure 6, the dimension of time taking the place of the dimension of temperature. The relation would be clearer if the relaxation were being studied at constant temperature (annealing) rather than during upscan of temperature.

On the other hand, a realization of the long time scale viscosity (or relaxation time) vs temperature behavior depicted in Figure 15b may be possible for samples of nanoscopic dimensions. The properties of water in the "nanopools" in hydrated hydrophilic polymers, whose study was pioneered by Johari and co-workers,[222] seem to be very close to that anticipated from the analysis provided in this section. This question remains to be evaluated by investigation of a wider range of nanosamples than have been studied to date. In particular, the study of hyperquenched microemulsions of water-in-oil type, in which the nanosample is separated from the nonaqueous components by a phase boundary (admittedly of complex form), should be easy to perform and instructive to examine. A study carried out using a variety of surfactants to separate the behavior of the water from that of the surface phase could add much to our understanding of this endlessly fascinating substance. Thermal annealing, and also upscanning studies of the Figure 6 type, are not limited to ambient conditions but could also be carried out on the pressurized material, in which case a wider range of behavior should be observable, possibly including behavior above the real T_g. Much remains to be done.

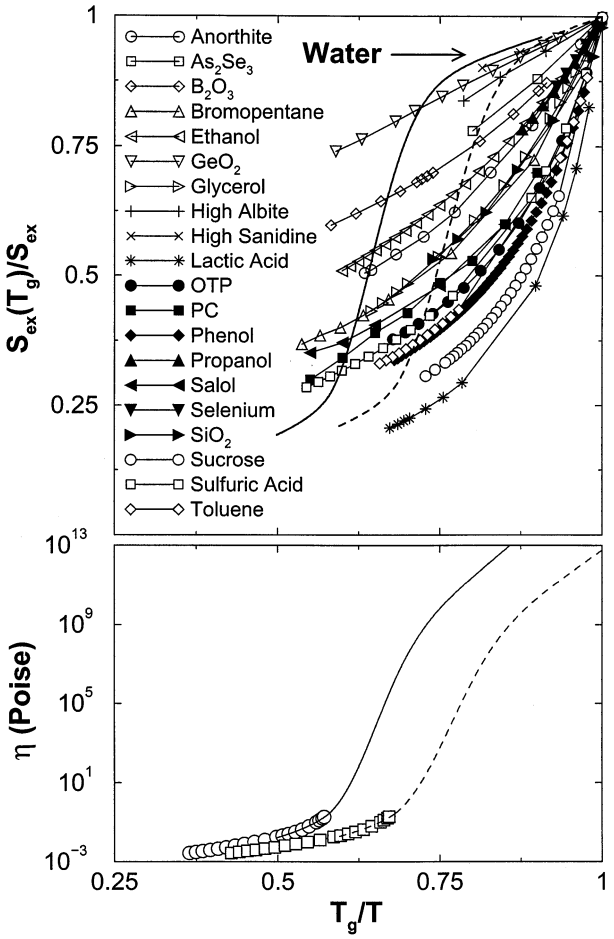

Figure 15. (a) The rate at which the entropy increases above its value at the glass transition with increasing temperature above the glass transition, using reciprocal temperature to aid comparison with the scaled Arrhenius plots for transport properties. For water, two curves are shown one for each of the *T*g scaling parameters 136 K and (new assignment) 165 K. The abnormal behavior of water is obvious. (b) Arrhenius plots for water viscosity, based on the use of each of the two entropy vs temperature relations shown in part a in the Adam Gibbs equation for viscosity. The other parameters of the Adam-Gibbs equation are obtained by the best fit of the available data in the temperature regime above 235 K.

IV. Concluding Remarks

In this article, we have not attempted to review the many sophisticated theoretical attempts to interpret the origin of the unusual physical properties of water (and its tetrahedral liquid relatives). Rather, we have confined ourselves to reviewing the limited physical behavior indicated by the article title requested by the editor of this thematic issue. These aspects have not been the subject of the searching and repeated studies that characterize much of water science. This is because of the relatively unpopular nature of supercooled liquid studies until recent times. However, the richness of the phenomenology found in these low temperature regions, in which entropy loses its dominance and subtle structural

effects can be manifested, is changing the outlook. It is likely that there will appear in the future an increasing interest in sorting out the many differences in opinion, not to say data, that exist at this time in the science of supercooled and glassforming aqueous solutions.

V. Acknowledgments

This work has been carried out under the auspices of the NSF, Solid State Chemistry Grant No. DMR 0082535. Thanks are due to Felix Franks and anonymous reviewers for critical comments that have improved this review. Special thanks are due to Francis Starr who provided a modified version of figures in his article (ref 112) especially for incorporation in this review.

Note Added in Proof

The revised value of T_g for water (see Section II.b.i, paragraph 10) has now been verified by duplicating the so-called "T_g of water" seen in Figure 5, using *noncrystallizing* glasses that have been hyperquenched and then annealed below T_g, in the manner used by Johari et al. to obtain the Figure 5 data. In a report just submitted to *Nature*, and posted on the (former Los Alamos, now Cornell) Physics Website http://arXiv.org/abs/physics/0207048. Yue and Angell have identified the source of the Figure 5 endotherm as a "shadow glass transition" that occurs well below the standard glass temperature. It is an annealing effect that, in noncrystallizing systems, precedes a crossover to a residual exotherm which is only then followed by the glass transition, in a delayed form. In the case of water this latter part of the thermogram is pre-empted by crystallization. The shadow effect occurs about 20% below the normal T_g, depending on details of the annealing treatment.

VI. References

(1) Seyler, R. J., Ed. *Assignment of the Glass Transition*, ASTM STP 1249, Am. Soc. Testing and Materials: Philadelphia, 1994; pp 32−49.
(2) Angell, C. A. In *Pergammon Encyclopedia of Materials: Science and Technology*; Buschow, K. H. J., Cahn, R. W., Flemings, M. C., Ilschner, B., Kramer, E. J., Mahajan, S., Eds.; Elsevier: New York, 2001; Vol. 4, pp 3565−3575.
(3) (a) Angell, C. A. In *Relaxations in Complex Systems*; Ngai, K., Wright, G. B., Eds.; National Technical Information Service, U.S. Department of Commerce, Springfield, VA, 1985, p 1. (b) Angell, C. A. *J. Non-Cryst. Solids* **1991**, *13*, 131−133. (c) Angell, C. A. *Science* **1995**, *267*, 1924.
(4) Sugisaki, M.; Suga, S.; Seki, S. *J. Chem. Soc. Jpn.* **1968**, *41*, 2591.
(5) MacMillan, J. A., Los, S. C. *J. Chem. Phys.* **1965**, *42*, 829.
(6) Ghormley, J. A. *J. Chem. Phys.* **1967**, *48*, 503; Ghormley, J. A. *J. Chem. Phys.* **1965**, *42*, 829.
(7) MacFarlane, D. R.; Angell, C. A. *J. Phys. Chem.* **1984**, *88*, 759.
(8) Johari, G. P.; Hallbrucker, A.; Mayer, E. *Nature* **1987**, *330*, 552.
(9) Mayer, E.; Hallbrucker, A.; Sartor, G.; Johari, G. P. *J. Phys. Chem.* **1995**, *99* (14), 5161.
(10) Johari, G. P. *J. Chem. Phys.* **1996**, *105*, 707.
(11) Fisher, M.; Devlin, J. P. *J. Phys. Chem.* **1995**, *99*, 11584.
(12) Ito, K.; Moynihan, C. T.; Angell, C. A. *Nature* **1999**, *398*, 492.
(13) Scott, R. S.; Kay, B. D. *Nature* **1999**, *398*, 788.
(14) Velikov, V.; Borick, S.; Angell, C. A. *Science* **2001**, *294*, 2335.
(15) Bentor, Y. K. *Geochim. Cosmochim. Acta* **1961**, *25*, 239.
(16) Moynihan, C. T.; Macedo, P. B.; Montrose, C. J.; Gupta, P. K.; DeBolt, M. A.; Dill, J. F.; Dom, B. E.; Drake, P. W.; Easteal, A. J.; Elterman, P. B.; Moeller, R. P.; Sasabe, H. A.; Wilder, J. A. *Ann. NY. Acad. Sci.* **1976**, *279*, 15.
(17) Ediger, M. D.; Angell, C. A.; Nagel, S. R. *J. Phys. Chem.* **1996**, *100*, 13200.
(18) Angell, C. A.; Ngai, K. L.; McKenna, G. B.; McMillan, P. F.; Martin, S. W. *Rev. Appl. Phys.* **2000**, *88*, 3113.
(19) Debenedetti, P. G. *Metastable Liquids*; Princeton Press: Princeton, NJ, 1996.
(20) Angell, C. A.; Tucker, J. C. *J. Phys. Chem.* **1980**, *84*, 268.
(21) Moynihan, C. T. *J. Chem. Educ.* **1967**, *44*, 531.
(22) (a) Ambrus, J. H.; Dardy, H.; Moynihan, C. T. *J. Phys. Chem.* **1972**, *76*, 3495. (b) Ambrus, J. H.; Moynihan, C. T.; Macedo, P. B. *J. Electrochem. Soc.* **1972**, *119*, 192.
(23) (a) Gammell, P. M.; Meister, R. *J. Chem. Phys.* **1976**, *64* (11), 4287−4292.
(24) (a) Angell, C. A. *J. Phys. Chem.* **1966**, *70*, 2793. (b) Angell, C. A.; Sare, E. J. *J. Chem. Phys.* **1970**, *52*, 1058. (c) Angell, C. A.; Bressel, R. D. *J. Phys. Chem.* **1972**, *76*, 3244. (d) Angell, C. A.; Donnella, J. *J. Chem. Phys.* **1977**, *67*, 4560.
(25) Xu, Y.; Hepler, L. G. *J. Chem. Thermodyn.* **1993**, *25*, 19.
(26) (a) Angell, C. A. In *Proc. Int. School of Physics*, "Enrico Fermi" Course CXXXIV; Mallamace, F., Stanley, H. E., Eds.; IOS Press Amsterdam, 1997, p 571. (b) Velikov, V.; Lu. Q.; Angell, C. A., to be published.
(27) Moynihan, C. T.; Easteal, A. J.; DeBolt, M. A.; Tucker, J. *J. Am. Ceram. Soc.* **1976**, *59*, 12; Moynihan, C. T.; Easteal, A. J.; DeBolt, M. A.; Tucker, J. *J. Am. Ceram. Soc.* **1976**, *59*, 16.
(28) Moynihan, C. T.; Balitactac, N.; Boone, L.; Litovitz, T. A. *J. Chem. Phys.* **1971**, *55*, 3013.
(29) Moynihan, C. T.; Bressel, R. D.; Angell, C. A. *J. Chem. Phys.* **1971**, *55*, 4414.
(30) Ambrus, J. H.; Moynihan, C. T.; Macedo, P. B. *J. Phys. Chem.* **1972**, *76*, 3287.
(31) (a) Silence, S. M.; Goates, S. R.; Nelson, K. A., *J. Non-Cryst. Solids* **1991**, *131−133*, 37. (b) Yan, Y.-X.; Cheng, L.-T.; Nelson, K. A. *J. Chem. Phys.* **1988**, *88*, 6477. (c) Halalay, I. C.; Nelson, K. A. *J. Non-Cryst. Solids* **1991**, *131−133*, 192.
(32) Madokoro, Y.; Yamamuro, O.; Yamasaki, H.; Matsuo, T.; Tsukushi, I.; Kamiyama, T.; Ikeda, S. *J. Chem. Phys.* **2002**, *116*, 5673.
(33) (a) Dupuy, J.; Chieux, P.; Calemczuk, R.; Jal, J. F.; Ferradou, C.; Wright, A.; Angell, C. A. *Nature* **1982**, *296*, 138−140. (b) Elarbyaouizerat, A.; Chieux, P.; Claudy, P.; Dupuy, J.; Jal, J. F.; Letoffe, J. M. *J. Phys.* (Paris) **1985**, *46* (C-8), 629−633.
(34) (a) MacFarlane, D. R.; Kadiyala, R. K.; Angell, C. A. *J. Phys. Chem.* **1983**, *87*, 235. (b) MacFarlane, D. R.; Scheirer, J.; Smedley, S. I. *J. Phys. Chem.* **1986**, *90*, 2168.
(35) Kanno, H. *J. Phys. Chem.* **1987**, *91*, 1967.
(36) Tammann, G. *Der Glasszustand*, 12, Scopola Voss, Leipzig, 1933.
(37) Vuillard, G. *Ann. Chim. Phys.* (Paris) **1957**, *2*, 223.
(38) Angell, C. A.; Sare, E. J. *J. Chem. Phys.* **1968**, *49* (10), 4713.
(39) Shalaev, E. Y.; Johnson-Elton, T. D.; Chang, L. Q.; Pikal, M. J. *Pharmaceut. Res.* **2002**, *19* (2), 195−201.
(40) (a) Kanno, H.; Shimada, K.; Katoh, T. *J. Phys. Chem.* **1989**, *93* (12), 4981−4985. (b) Kanno, H.; Ohnishi, A.; Tomikawa, K. et al. *J. Raman Spectrosc.* **1999**, *30* (8), 705−713.
(41) Oguni, M.; Angell, C. A. *J. Chem. Phys.* **1980**, *73*, 1948.
(42) Rasmussen, D. H.; Mckenzie, A. P. *J. Phys. Chem.* **1968**, *220*, 1315.
(43) Ghormley, J. A. *J. Am. Chem. Soc.* **1957**, *79*, 1862.
(44) Jabrane, S.; Letoffe, J. M.; Claudy, P. *Thermochim. Acta* **1998**, *311* (1−2), 121−127.
(45) Boehm, L.; Smith, D. L.; Angell, C. A. *J. Mol. Liq.* **1987**, *36*, 153.
(46) Boutron, P.; Kaufman, A. *Cryobiology* **1970**, *16*, 557.
(47) Slie, W. M.; Donfor, A. R., Jr.; Litovitz, T. A. *J. Chem. Phys.* **1966**, *44*, 3712.
(48) (a) Shalaev, E. Y.; Franks, F. *Thermochim. Acta* **1995**, *255*, 49. (b) Franks, Felix, private communication.
(49) (a) Crowe, J. H.; Crowe, L. M.; Mouradian, R. *Cryobiology* **1983**, *20*, 346. (b) Crowe, J. H.; Crowe, L. M. *Biol. Membr.* **1984**, *5*, 57.
(50) Green, J. L.; Angell, C. A. *J. Phys. Chem.* **1989**, *93*, 2880.
(51) Yannas, I. *Science* **1968**, *160*, 298.
(52) Rasmussen, D. H.; Mackenzie, A. P. *J. Phys. Chem.* **1968**, *72*, 1315; Rasmussen, D. H.; Mackenzie, A. P. *J. Phys. Chem.* **1971**, *75*, 967.
(53) Kanno, H.; Speedy, R. J.; Angell, C. A. *Science* **1975**, *189*, 880.
(54) Glycerol is normally pumped around chemical plants in which it is manufactured in liquid form, although the melting point is 291 °C. However, it is a matter of experience that if ever crystallization should occur, the entire piping system has to be replaced as it will always occur again in a short time even after the whole system has been exposed to temperatures far above the melting point.
(55) Mishima, O.; Susuki, Y. *J. Chem. Phys.* **2001**, *115*, 4199.
(56) (a) Kanno, H.; Angell, C. A. *J. Phys. Chem.* **1977**, *81*, 2639. (b) Kanno, H.; Angell C. A., unpublished work.
(57) (a) Kanno, H.; Satoh, H. *Bull. Chem. Soc. Jpn.* **1985**, *58*, 2487. (b) Kanno, H.; Shimada, K.; Yoshino, K.; Iwamata, T. *Chem. Phys. Lett.* **1984**, *112*, 242.

(58) Fahy, G. M. In *Organ Preservation, Present and Future*; Pegg, D. E., Jacobsen, I. A., Halasz, N. A., Eds.; MTP Press: Lancaster, 1981.
(59) Pegg, D. E., Karow, A. M., Eds. *The Biophysics of Cryopreservation*; Plenum Press: New York, 1987; pp 147−171.
(60) See, for instance, symposium papers in *J. Microscop. 141*, 1986.
(61) (a) Baudot, A.; Boutron, P. *Cryobiology* **1998**, *37* (3), 187−199. (b) Boutron, P.; Kaufman, A. *Cryo-Lett.* **1978**, *15*, 93.
(62) Fahy, G. M.; MacFarlane, D. R.; Angell, C. A.; Meryman, H. T. *Cryobiology* **1984**, *21*, 407−426.
(63) (a) MacFarlane, D. R.; Angell, C. A.; Fahy, G. M. *Cryoletters* **1981**, *2*, 353−358. (b) Macfarlane, D. R.; Forsyth, M. *Cryo-Lett.* **1989**, *10*, 139.
(64) Boutron, P. *Cryobiology* **1990**, *27*, 55.
(65) Levine, H.; Slade, L. *Biopharm.* **1992**, *5*, 36.
(66) Crowe, L. M.; Crowe, J. H.; Rudolph, A.; Womersley, C.; Appel, L. *Arch. Biochem. Biophys.* **1985**, *242*, 240.
(67) Miller, D. P.; de Pablo, J. J.; Corti, H. *Pharm. Res.* **1997**, *14*, 578.
(68) Kuleshova, L. L.; MacFarlane, D. R.; Trounson, A. O.; Shaw, J. M. *Cryobiology* **1999**, *38* (2), 119−130.
(69) Aldous, B. J.; Auffret, A. D.; Franks, F. *Cryo-Lett.* **1995**, *16*, 181.
(70) Sputtek, A.; Singbartl, G.; Langer, R.; Schleinzer, W.; Henrich, H. A.; Kuhnl, P. *Cryo-Lett.* **1995**, *16*, 283.
(71) Macfarlane, D. R.; Forsyth, M. *Cryobiology* **1990**, *27*(4), 345.
(72) Wolfe, J.; Bryant, G. *Cryobiology* **1999**, *39*, 103.
(73) Pegg, D. E. *Cryo-Lett.* **2001**, *22* (2), 105.
(74) Onadera, N.; Suga, H.; Seki, S. *Bull. Chem. Soc. Jpn.* **1968**, *41*, 2222.
(75) Salecki-Gerhardt, A.; Stowell, J. G.; Byrn, S. R.; Zografi, G. *J. Pharm. Sci.* **1996**, *84*, 318.
(76) Ding, S.-P.; Fan, J.; Green, J. L.; Lu, Q.; Sanchez, E.; Angell, C. A. *J. Therm. Anal.* **1996**, *47*, 1391.
(77) (a) Mishima, D.; Calvert, L. D.; Whalley, E. *Nature* **1984**, *310*, 393−395. (b) Mishima, D.; Calvert, L. D.; Whalley, E. *Nature*, **1985**, *314*, 76. (c) Mishima, O.; Takemure, K.; Aoki, K. *Science* **1991**, *254*, 406.
(78) Mishima, O. *J. Chem. Phys.* **1994**, *100*, 5910.
(79) Sciortino, F.; Essman, U.; Stanley, H. E.; Hemmati, M.; Shao, J.; Wolf, G. H.; Angell, C. A. *Phys. Rev. E* **1995**, *52*, 6484.
(80) (a) Jenniskens, P.; Blake, D. F. *Science* **1994**, *265*, 753. (b) Jenniskens, P.; Barnhak, S. F.; Blake, F.; McCoustra, M. R. S. *J. Chem. Phys.* **1997**, *107*, 1232.
(81) Sceats, M. G.; Rice, S. A. In *Water: A Comprehensive Treatis*; Franks, F., Ed. Plenum Press: London, 1982; Vol. 7, pp 83−211.
(82) (a) Burton, E. F.; Oliver, W. F. *Nature* **1935**, *135*, 505. (b) Burton, E. F.; Oliver, W. F. *Proc. R. Soc.* (London), **1935**, *A153*, 166.
(83) Heide, H.-G.; Zeitler, E. *Ultramicroscopy* **1985** *16*, 151.
(84) Pryde, J. A.; Jones, G. O. *Nature* **1952**, *170*, 635.
(85) Hallbrucker, A.; Mayer E.; Johari, G. P. *J. Phys. Chem.* **1989**, *93*, 4986.
(86) Olander, D. S.; Rice, S. A. *Proc. Nat. Acad. Sci. U.S.A.* **1972**, *69*, 98.
(87) (a) Brüeggeller, P.; Mayer, E. *Nature* **1980**, *288b*, 569. (b) Brüeggeller, P.; Mayer, E. *Nature* **1982**, *298*, 715.
(88) Dubochet, J.; McDowell, A. W. *J. Microsc.* **1981**, *124*, RP3.
(89) Mayer, E.; Pletzer, R. *J. Chem. Phys.* **1984**, *80*, 2939.
(90) Mayer, E. *J. Appl. Phys.* **1985**, *58*, 663; Mayer, E. *J. Microsc.* **1985**, *140*, 3; Mayer, E. *J. Microsc.* **1986**, *141*, 269.
(91) Fleissner, G.; Hallbrucker, A.; Mayer, E. *J. Phys. Chem.* **1998**, *B102*, 6239.
(92) Hallbrucker, A.; Mayer, E.; Johari, G. P. *Philos. Mag.* **1989**, *B60*, 179.
(93) Hallbrucker, A.; Mayer, E. *J. Phys. Chem.* **1987**, *91*, 503.
(94) Johari, G. P.; Hallbrucker, A.; Mayer, E. *J. Phys. Chem.* **1989**, *93*, 2648.
(95) Hallbrucker, A.; Mayer, E.; Johari, G. P. *J. Phys. Chem.* **1989**, *93*, 4986.
(96) Klug, D. D.; Handa, Y. P. *J. Phys. Chem.* **1988**, *92*, 3323.
(97) Hallbrucker, A.; Mayer, E.; Johari, G. P. *J. Phys. Chem.* **1989**, *93*, 7751.
(98) Johari, G. P.; Hallbrucker, A.; Mayer, E. *Science* **1996**, *273*, 90.
(99) DeBolt, M. A.; Easteal, A. J.; Macedo, P. B.; Moynihan, C. T. *J. Am. Ceram. Soc.* **1976**, *59*, 16−21.
(100) (a) Hodge, I. M. *J. Non-Cryst. Solids* **1994**, *169*, 211−266. (b) Scherer, G. W. *Relaxation in Glass and Composites*; Wiley and Sons: New York, 1986; Chapter 10.
(101) McCrum, M. G.; Reid, B. E.; Williams, G. *Anelastic and Dielectric Effects in Polymeric Solids*; Wiley: London, New York, 1967; Chapter 1.
(102) Richert, R.; Angell, C. A. *J. Chem. Phys.* **1998**, *108*, 9016.
(103) Yue, Y.-Z.; Angell, C. A., to be published.
(104) (a) Huang, J.; Gupta P. K. *J. Non-Cryst. Solids* **1992**, *151*, 175. (b) Ram, S.; Johari, G. P. *Philos. Mag.* **1990**, *61*, 299. (c) Chen, H. S.; Coleman, E. *Applied Phys. Lett.* **1976**, *28*, 245. (d) Yue, Y.-Z.; Christiansen, J. deC.; Jensen, S. L. *Chem. Phys. Lett.* **2002**, *357*, 20, and to be published.
(105) Buch, V., private communication.
(106) Hage, W.; Hallbrucker, A.; Mayer, E.; Johari, G. P. *J. Chem. Phys.* **1994**, *100*(4), 2743.
(107) Smith, R. S.; Huang, C.; Wong, E. K. L.; Kay, B. D. *Surf. Sci. Lett.* **1996**, *367*(1), L13.
(108) Jenniskens, P.; Blake, D. F. *Astrophys. J.* **1996**, *473*(2), 1104, Part 1.
(109) (a) Doremus, R. H. *Rates of Phase Transformations*; Academic: New York, 1985; Chapter II. (b) Christian, J. W. *The Theory of Transformation in Metals and Alloys*, 2nd ed.; Pergammon Press: Oxford, 1975.
(110) Ngai, K. L.; Magill, J. H.; Plazek, D.; J. *J. Chem. Phys.* **2000**, *112*, 1887.
(111) Ito, K.; Moynihan, C. T.; Angell, C. A. *Nature* **1999**, *398*, 492−495.
(112) Starr, F. W.; Angell, C. A.; Stanley, H. E. http://xxx.lanl.gov/abs/cond-matt? 9903451., revised form submitted to *J. Chem. Phys.*
(113) Johari, G. P. *J. Phys. Chem. B* **1998**, *102*, 4711.
(114) Narten, A. H.; Venkatesh, C. G.; Rice, J. A. *J. Chem. Phys.* **1976**, *64*, 1106.
(115) Vollmayr, K.; Kob, W.; Binder, K. *Phys. Rev. B.* **1996**, *54*, 15808.
(116) (a) Hemmati, M.; Moynihan, C. T.; Angell, C. A. *J. Chem. Phys.* **2001**, *115* (14), 6663−6671. (b) Angell, C. A.; Bressel, R. D.; Hemmatti, M.; Sare, E. J.; Tucker, J. C. *Phys. Chem. Chem. Phys.* **2000**, *2*, 1599−1566.
(117) (a) Easteal, A. J.; Angell, C. A. *J. Phys. Chem.* **1970**, *74*, 3987. (b) Easteal, A. J.; Angell, C. A. *J. Chem. Phys.* **1972**, *56*, 4231.
(118) Vogel, W.; Gerth, K. *Glastech. Ber.* **1958**, *31*, 15; Vogel, W.; Gerth, K. *Silicattech.* **1958**, *9*, 495.
(119) Dobrokhotova, Zh. V.; Zakharova, B. S. *Inorg. Mater.* **2000**, *36*, 191, translated from the Russian original.
(120) (a) Angell, C. A.; Bressel, R. D.; Green, J. L.; Kanno, H.; Oguni, M.; Sare, E. J. *Int. J. Food Sci.* **1994**, *22*, 115−142. (b) Oguni, M.; Angell, C. A., unpublished work.
(121) Liu, L.-G.; Ringwood, A. E. *Earth Planet. Sci. Lett.* **1975**, *28*, 209.
(122) (a)Wolf, G. H.; Wang, S.; Herbst, C. A., Durben, D. J.; Oliver, W. J.; Kang, Z. C.; Halvorsen, C. In *High-Pressure Research: Application to Earth and Planetary Sciences*; Manghnani, Y. S., Manghnani, M. H., Eds.; Terra Scientific Publishing Co./Am. Geophysical Union: Tokyo/Washington, 1992. (b) Williams, Q.; Knittle, R.; Reichlin, R.; Martin, S.; Jeanloz, R. *Science* **1990**, *249*, 647.
(123) (a) Poole, P. H.; Sciortino, F.; Essmann, U.; Stanley, H. E. *Nature* (London) **1992**, *360*, 324. (b) Poole, P. H.; Sciortino, F.; Essmann, U.; Stanley, H. E. *Phys. Rev. E* **1993**, *48*, 4605.
(124) Yamada, M.; Mossa, S.; Stanley, H. E.; Sciortino, F. *Phys. Rev. Lett.*, in press, http://xxx.lanl.gov/pdf/cond-mat/0202094.
(125) Starr, F., Ph D. Thesis, Boston University, 1999.
(126) Alamoudi, A.; Dubochet, J.; Studer, D., submitted for publication.
(127) MacFarlane, D. R.; Angell, C. A. *J. Phys. Chem.* **1982**, *86*, 1927.
(128) Mishima, O. *Nature* **1996**, *384*, 546.
(129) (a) Schober, H.; Koza, M.; Tölle, A.; Fujara, F.; Angell, C. A.; Bohmer, R. *Physica B* **1998**, *241−243*, 897−902. (b) Agladze, N. I.; Sievers, A. J. *Phys. Rev. Lett.* **1998**, *80*, 4209.
(130) Koza, M.; Tölle, A., Schober, H.; Fujara, F., unpublished work.
(131) (a) Sokolov, A. P.; Rossler, E.; Kisliuk, A.; Quittman, D. *Phys. Rev. Lett.* **1993**, *71*, 2062. (b) Frick, B.; Richter, D. *Science* **1995**, *267*, 1939. (c) Angell, C. A.; Ngai, K. L.; McKenna, G. B.; McMillan, P. F.; Martin, S. W. *Rev. Appl. Phys.* **2000**, *88*, 3113.
(132) Liu, X. et al. *Phys. Rev. Lett.* **1997**, *78*, 4418.
(133) Mishima, O.; Stanley, H. E. *Nature* **1998**, *392*, 164.
(134) Mishima, O.; Stanley, H. E. *Nature* **1998**, *396*, 329.
(135) Mishima, O. *Phys. Rev. Lett.* **2000**, *85*, 334−336.
(136) Lang, E.; Ludemann, H. D. *J. Chem. Phys.* **1977**, *67*, 718.
(137) Lang, E. W.; Lüdemann, H. D. *Angew. Chem., Int. Ed. Engl.* **1982**, *21*, 315.
(138) (a) Angell, C. A.; Borick, S.; and Grabow M.; *J. Non-Cryst. Solids*, **1996**, 205−207, 463−471. (b) Sastry, S.; Angell, C. A., to be published.
(139) McFarlane, D. R. *Cryobiology* **1986**, *23*, 230.
(140) Hsich, S. Y.; Gammon, R. W.; Montrose, C. J. *J. Chem. Phys.* **1972**, *56*, 1666.
(141) Dupuy, J.; Chieux, P.; Calemczuk, R.; Jal, J. F.; Ferradou, C.; Wright, A.; Angell, C. A. *Nature* **1982**, *296*, 138−140.
(142) de Neufville, J.; Turnbull, D. *Discuss. Faraday Soc.* **1970**, *50*, 182.
(143) Mishima, O. *Phys. Rev. Lett.* **2000**, *85*, 1322.
(144) (a) Uhlmann, D. R. In *Amorphous Solids*, Douglas, R. W., Ellis, D., Eds.; Wiley and Sons: New York, 1971; Chapter 22, pp 205−214. (b) Uhlmann, D. R. *J. Non-Cryst. Solids* **1972**, *7*, 237.
(145) (a) Angell, C. A.; Dworkin, A.; Figuiere, P.; Fuchs, A.; Szwarc, H. *J. Chim. Phys.* **1985**, *82*, 773. (b) Stickel, F.; Fischer, E. W.; Richert, R. *J. Chem. Phys.* **1995**, *102*, 6251; Stickel, F.; Fischer, E. W.; Richert, R. **1996**, *104*, 2043. (c) Angell, C. A.; Monnerie, L.; Torell, L. M. *Symp. Mater. Res. Soc.* O'Reilly, J. M., Ed. **1991**, *215*, 3−9.
(146) Ferrer, M. L.; Sakai, H.; Kivelson, D.; Alba-Simeonesco, C. *J. Phys. Chem.* **1999**, *103*, 4191.

(147) Williams, E.; Angell, C. A. *J. Polym. Sci., Polym. Lett.* **1973**, *11*, 383.
(148) Cohen, M. H.; Turnbull, D. *J. Chem. Phys.* **1959**, *31*, 1164.
(149) Macedo, P. B.; Moynihan, C. T.; Bose, R. A. *Phys. Chem. Glasses* **1972**, *13*, 171.
(150) Moynihan, C. T.; Balitactac, N.; Boone, L.; Litovitz, T. A. *J. Chem. Phys.* **1971**, *55*, 3013.
(151) Wu, L.; Dixon, P. K.; Nagel, S. R.; Williams, B. D.; Carini, J. P. *J. Non-Cryst. Solids* **1991**, *131*−*133*, 32.
(152) Angell, C. A. *Annu. Rev. Phys. Chem.* **1992**, *43*, 693.
(153) Kauzmann, W. *Chem. Rev.* **1948**, *43*, 218.
(154) (a) Stillinger, F. H. *J. Chem. Phys.* **1988**, *88*, 7818. (b) Stillinger, F. H.; Debenedetti, P. G.; Truskett, T. M. *J. Phys. Chem.* **2001**, *105*, 11809.
(155) Angell, C. A.; Richards, B. E.; Velikov, V. *J. Phys.: Condens. Matter* **1999**, *11*, A75−A94.
(156) Johari, G. P. *J. Chem. Phys.* **2000**, *113*, 1, and references therein.
(157) Böhmer, R.; Angell, C. A. In *Disorder Effects on Relaxation Processes*; Blumen, A., and Richert, R., Eds.; Springer: Berlin, 1994; p 11.
(158) Richert, R.; Angell, C. A. *J. Chem. Phys.* **1998**, *108*, 9016.
(159) (a) Böhmer, R.; Angell, C. A. *Phys. Rev. B.* **1992**, *45*, 10091−10094. (b) Böhmer, R.; Ngai, K. L.; Angell, C. A.; Plazek, D. J. *J. Chem. Phys.* **1993**, *99* (5), 4201−4209. (c) Plazek, D. J.; Ngai, K. L. *Macromolecules* **1991**, *24*, 1222.
(160) Wang, L.; Velikov, V.; Angell, C. A. *J. Chem. Phys.*, submitted for publication.
(161) Green, J. L.; Ito, K.; Xu, K.; Angell, C. A. *J. Phys. Chem. B.* **1999**, *103*, 3991.
(162) Martinez, L.-M.; Angell, C. A. *Nature* **2001**, *410*, 663.
(163) (a) Sastry, S.; Debenedetti, P. G.; Stillinger, F. H. *Nature* **1998**, *393*, 554. (b) Sastry, S. *Nature* **2001**, *409*, 164.
(164) Stillinger, F. H.; Debenedetti, P. G. *Nature* **2001**, *410*, 259.
(165) Scala, A.; Angelani, L.; Di Leonardo, R.; Ruocco, G.; Sciortino, F.; *Philos. Mag.* **2002**, *82*, 151.
(166) Velikov, V.; Angell, C. A., unpublished work.
(167) Bressel, R. D. Ph.D. Thesis, Purdue University, 1971.
(168) Saika-Voivod, I.; Poole, P. H.; Sciortino, F. *Nature* **2001**, *412*, 514.
(169) Angell, C. A. *J. Phys. Chem.* **1993**, *97*, 6339.
(170) Starr, F. W.; Angell, C. A.; Stanley, H. E.*J. Chem. Phys.*, manuscript under review.
(171) Williams, E.; Angell, C. A. *J. Phys. Chem.* **1977**, *81*, 232.
(172) Jäckle, E. *Rep. Prog. Phys.* **1986**, *49*, 171.
(173) Angell, C. A.; Tucker, J. C. *J. Phys. Chem.* **1974**, *78*, 278.
(174) (a) Karger, N.; Lüdemann, H.-D. *Z. Naturforsch* **1991**, *46c*, 313−17. (b) Karger, N.; Vardag, T.; Ludemann, H.-D. *J. Chem. Phys.* **1990**, *93*, 3437.
(175) (a) Girlich, D.; Lüdemann, H.-D.; Buttersack, C.; Buchholz, K. *Z. Naturforsch.*, Teil C, **1994**, *49*, 258. (b) Heinrich-Schramm, A.; Buttersack, C.; and Lüdemann, H.-D. *Carbohydr. Res.* **1996**, *293*, 205. (c) Rampp, M.; Buttersack, C.; Lüdemann H.-D. *Carbohydr. Res.* **2000**, *328*, 561.
(176) Miller, D. P.; Conrad, P. B.; Fucito, S., et al., *J. Phys. Chem.* **2000**, *B104*, 10419.
(177) Shamblin, S. L.; Tang, X.; Chang, L.; Hancock, B. C.; Pikal, M. *J. Phys. Chem. B* **1999**, *103*, 4113.
(178) Oguni, M.; Angell, C. A., unpublished work.
(179) Angell, C. A.; MacFarlane, D. R.; Oguni, M. *Ann. N. Y. Acad. Sci.* **1986**, *484*, 241.
(180) (a) Bengtzelius, U.; Götze, W.; Sjölander, A., *J. Phys. Chem.* **1984**, *17*, 5915. (b) Götze, W.; Sjögren, L. *Rep. Prog. Phys.* **1992**, *55*, 55. (c) Taborek, P.; Kleinman, R. N.; Bishop, D. *J. Phys. Rev.* **1986**, *B34*, 1835.
(181) Doolittle, A. K. *J. Appl. Phys.* **1951**, *22*, 1471.
(182) Adam, G.; Gibbs, J. H *J. Chem. Phys.* **1965**, *43*, 139.
(183) Gibbs, J. H.; Dimarzio, E. A. *J. Chem. Phys.* **1958**, *28*, 373.
(184) (a) Macedo, P. B.; Capps, W.; Litovitz, T. A. *J. Chem. Phys.* **1966**, *44*, 3357. (b) Leidecker, H. W.; Macedo, P. B.; Litovitz, T. A. *O. N. R. Technol. Rept. No. 1* **1969**, N00014−68-A-0506−0021.
(185) (a) Angell, C. A.; Wong, J. *J. Chem. Phys.* **1970**, *53*, 2053. (b) Angell, C. A. *J. Phys. Chem.* **1971**, *75*, 3698. (c) Angell, C. A.; Rao, K. J. *J. Chem. Phys.* **1972**, *57*, 470.
(186) Perez, J. *J. Phys.* **1985**, *46*, C10, 427.
(187) (a) Ponyatovsky, E. G.; Sinitsyn, V. V. *Physica B* **1997**, *265*, 121. (b) Moynihan, C. T. *Mater. Res. Soc. Symp. Proc.* **1997**, *455*, 411. (c) Angell, C. A.; Moynihan, C. T. *Met. Mater. Trans.* **2000**, *31B*, 587. (d) Granato, A. V. *Phys. Rev. Lett.* **1992**, *68*, 974.
(188) (a) Sastry, S.; Sciortino, S.; Stanley, H. E. *Chem. Phys. Lett.* **1993**, *207*, 275. (b) Stanley, H. E.; Blumberg, R. L.; Geiger, A.; Mausbach, P.; Teixeira, J. *J. Phys.* **1984**, *45* (NC-7) 3. (c) Geiger, A.; Stanley, H. E. *Phys. Rev. Lett.* **1982**, *49*, 1749. (d) Sciortino, F.; Geiger, A.; Stanley, H. E. *J. Chem. Phys.* **1992**, *96*, 3957.
(189) Sastry, S.; Sciortino, S.; Stanley, H. E. *J. Chem. Phys.* **1993**, *98*, 9863.
(190) Borick, S. S.; Debenedetti, P. G.; Sastry, S. *J. Phys. Chem.* **1995**, *99*, 3781.
(191) Sastry, S.; Debenedetti, P. G.; Sciortino, S.; Stanley, H. E. *Phys. Rev. E* **1996**, *53*, 6144.
(192) Rebelo, L. P. N.; Debenedetti, P. G.; Sastry, S. *J. Chem. Phys.* **1998**, *109*, 626.
(193) Tanaka, H. *J. Chem. Phys.* **1999**, *112*, 799.
(194) Kivelson, D.; Tarjus, G. *J. Phys. Chem.* **2001**, *105*, 6620.
(195) Stanley, H. E.; Teixeira, J. *J. Chem. Phys.* **1980**, *73*, 3404.
(196) Stanley, H. E.; Blumberg, R. L.; Geiger, A.; Mausbach, P.; Teixeira, J. *J. de Physique* **1984**, *45* (NC-7) 3.
(197) Geiger, A.; Stanley, H. E. *Phys. Rev. Lett.* **1982**, *49*, 1749.
(198) Sciortino, F.; Geiger, A.; Stanley, H. E. *J. Chem. Phys.* **1992**, *96*, 3957.
(199) Wunderlich, B. *J. Phys. Chem.* **1960**, *64*, 1052.
(200) Derrida, B. *Phys. Rev. Lett.* **1987**, *45*, 79; Derrida, B. *Phys. Rev. B.* **1981**, *24*, 2613.
(201) Speedy, R. J. *J. Phys. Chem. B* **1999**, *102*, 4060.
(202) (a) Buchner S.; Heuer, A. *Phys. Rev.* **1999**, *E 60*(6), 6507. (b) Sastry, S. *Nature* **2001**, *409*, 164.
(203) (a) Starr, F. W.; Sastry, S.; La Nave, E.; Stanley, H. E.; Sciortino, F. *Phys. Rev.* **2001** *E 63*. 041201 Part 1. (b) Scala, A.; Angelani, L.; Di Leonardo, R.; Ruocco, G.; Sciortino, F. *Philos. Mag.* **2002**, *82*, 151.
(204) Greet, R. J.; Turnbull, D. *J. Chem. Phys.* **1967**, *47*, 2185.
(205) Takahara, S.; Yamamuro, O.; Matsuo, T. *J. Phys. Chem.* **1995**, *99*, 9580.
(206) Angell, C. A.; Finch, E. D.; Woolf, L. A.; Bach, P. *J. Chem. Phys.* **1976**, *65*, 3063.
(207) Oguni, M.; Fujimori, H.; Oguni, M. *J. Chem. Therm.* **1994**, *26*, 367.
(208) Angell, C. A. *J. Res. NIST* **1997**, *102*, 171.
(209) Goldstein, M. *J. Chem. Phys.* **1969**, *51*, 3728.
(210) (a) Stillinger, F. H. *Science* **1995**, *267*, 1935. (b) Stillinger, F. H.; Weber, T. A. *Science* **1984**, *228*, 983. (c) Stillinger, F. H. *J. Chem. Phys.* **1984**, *80*, 2742.
(211) Giovambattista, N.; Starr, F. W.; Sciortino, F., et al. *Phys. Rev.* **2002**, *E 65* (4): art. no. 041502, Part 1.
(212) (a) Starr F. W.; Sastry, S.; La Nave, E. et al. *Phys. Rev.* **2001**, *E 63*, 041201, Part 1. (b) La Nave, E.; Scala, A.; Starr, F. W. et al. *Phys. Rev.* **2001**, *E64*, 036102, Part 2. (c) Saika-Voivod, I.; Sciortino, F.; Poole, P. H. *Phys. Rev.* **2001**, *E63*, 011202, Part 1.
(213) Greet, R. J.; Turnbull, D. *J. Chem. Phys.* **1967**, *47*, 2185.
(214) Takahara, S.; Yamamuro, O.; Matsuo, T. *J. Phys. Chem.* **1995**, *99*, 9580.
(215) Angell, C. A.; Finch, E. D.; Woolf, L. A.; Bach, P. *J. Chem. Phys.* **1976**, *65*, 3063.
(216) Oguni, M.; Fujimori, H.; Oguni, M. *J. Chem. Therm.* **1994**, *26*, 367.
(217) Angell, C. A. *J. Res. NIST* **1997**, *102*, 171.
(218) Angell, C. A.; Borick, S. *J. Non-Cryst. Solids*, in press.
(219) Speedy, R. J.; Debenedetti, P. G.; Smith, R. S.; Huang, C.; Kay, B. D. *J. Chem Phys.* **1996**, *105*(1), 240.
(220) Grabow, M. H.; Gilmer, G. H. *Mater. Res. Soc. Symp. Proc.* **1989**, *141*, 341.
(221) Filliponi, A.; Dicicco, A. *Phys. Rev. B* **1995**, *51*, 12322.
(222) (a) Hofer, K.; Mayer, E.; Johari, G. P. *J. Phys. Chem.* **1990**, *94*, 2689. (b) Hofer, K.; Mayer, E.; Johari, G. P. *J. Phys. Chem.* **1991**, *95*, 7100.
(223) It is the stress developed across the vitreous solid in the presence of a sharp temperature difference that causes inexpensive glass vessels to shatter when suddenly heated or cooled. By contrast with this behavior, the process of vitrification in pure silica glass can occur with so little change of volume that a white hot silica vessel can be dropped into a bucket of cold water without ill effect.
(224) Kim, W.-H.; McPhillen, M.; Hayes, J. M.; Small, G. J. *Chem. Phys. Lett.* **1993**, *207*, 443.
(225) Angell, C. A.; Alba, C.; Arzimanoglou, A.; Böhmer, R.; Fan, J.; Lu, Q.; Sanchez, E.; Senapati, H.; Tatsumisago, M. *Am. Inst. Phys. Conference Proceedings* No. 256, 3−19 (1992), (see Figure 9).
(226) Wang, L.-M.; Angell, C. A., to be published.

CR000689Q